Advances in Nano Research, *Vol. 14, No. 4 (2023) 335-353*
https://doi.org/10.12989/anr.2023.14.4.335

Vibration control, energy harvesting and forced vibration of the piezoelectric NEMS via paradox-free local/nonlocal theory

Zohre Moradi[1], Farzad Ebrahimi*[2] and Mohsen Davoudi[1]

[1]*Faculty of Engineering and Technology, Department of Electrical Engineering, Imam Khomeini International University, 34149-16818, Qazvin, Iran*
[2]*Faculty of Engineering, Department of Mechanics, Imam Khomeini International University, Qazvin, Iran*

(*Received January 24, 2021, Revised June 13, 2022, Accepted June 14, 2022*)

Abstract. The possibility of energy harvesting as well as controlled vibration of a three-layered beam consisting of two piezoelectric layer and one core layer made of nonpiezoelectric material is investigated using paradox-free local/nonlocal theory. The three-layered nanobeam is resting on an elastic foundation and subjected to a blast load. Also, the core layer is made of Nano-composites reinforced by CNTs and carbon fibers (MHCD). Governing equations as well as boundary conditions are obtained using Hamilton,s principle. The equations discretized by Generalized Differential Quadrature Method (GDQM) and solved by Newmark beta method. In addition, two differential and integral gains are employed for controlling the forced vibration. The size-dependency of the elastic foundation is considered using two-phase elasticity. The effect of elastic foundation, control gains, nonlocal factor, as well as parameters affecting the core material on the forced vibration and energy harvesting is investigated in detail. The equations as well as solution procedure is validated utilizing some compassion studies. This work can be a basis for future studies on energy harvesting and controlled vibration in small scales.
Keywords: energy harvesting; MHCD material; two-phase electric environment; vibration control

1. Introduction

Piezoelectric materials, due to their properties, may be utilized in smart devices (Bai *et al*. 2021, Lu *et al*. 2021, Zhou *et al*. 2021, Li *et al*. 2022a, b, Shen *et al*. 2022). The use of piezoelectric materials in nanodevices such as nanosensors (Wan *et al*. 2004), nanogenerators (Wang and Song 2006), and so on has lately gained attention. The scale of gadgets at these sizes is one of the most significant aspects that should be studied (Peng *et al*. 2021, Gao *et al*. 2022, Li *et al*. 2022c, Yu *et al*. 2022a, b, Zhang *et al*. 2022). Several academics have put forth a lot of time and effort to study the effects of size (Hamidi *et al*. 2015, Allahkarami *et al*. 2017, Ehyaei *et al*. 2017, Akbaş 2018a, b, Arefi and Zenkour 2018, Aydogdu *et al*. 2018, Bensaid *et al*. 2018, Navi *et al*. 2019, Ebrahimi *et al*. 2020b, Gafour *et al*. 2020, Matouk *et al*. 2020). To date, several theories, such as nonlocal elasticity (Eringen 1972, 1983, Eringen and Edelen 1972, Adhikari *et al*. 2015), have been proposed and used to account for the impact of size.

Since the introduction of integral nonlocal elasticity (Kröner 1967, Krumhansl 1968, Kunin 1968), numerous researchers have utilized this theory to investigate size-dependent devices. Following the development of differential form nonlocal elasticity of Eringen (1983), this theory became widely utilized due to the decrease in complexity and expense of calculation. Buckling, bending, and vibration of nanostructures, for example, were studied using various beam theories and differential nonlocal elastic (Reddy 2007). Wave propagation is studied using Euler-Bernoulli and nonlocal differential equations (Ebrahimi *et al*. 2018). Timoshenko beam theory and nonlocal differential theory were utilized to investigate the nonlinear vibration of piezoelectric nanobeams. However, the differential nonlocal theory has contradictions that make it untrustworthy for widespread use. For example, using differential, the initial natural frequency of a cantilever beam cannot be calculated correctly and precisely. As a result, academics attempted to eliminate paradoxes, one of which being Challamel and Wang (2008) study. According to Challamel *et al*. (2014), the initial vibration frequency of a cantilever nanobeam decreases as its nonlocality increases. Romano *et al*. (2017) studied bending features of cantilever nanobeams, and asserted that the incompatibility between the order of equations and the number of boundary conditions can be solved with two additional boundary conditions. Regarding this, hardening effect can be seen in aby type of boundary condition in a stress-driven model which was proposed by Romano and Barretta (2017). In addition, using this model and Euler Bernoulli beam theory, nanobeam vibration was probed by Apuzzo *et al*. (2017) which showed that the frequency of beams with this model in different boundary conditions can be increased.

Moreover, one of the most recent theory utilized to eradicate these inconstancies is two-phase local/nonlocal theory. Two-phase elasticity is of interest since the order of boundary conditions is compatible with order of the governing equations and the results are validated by the results obtained from integral model as well as molecular dynamics. Up to now, by utilizing two-phase theory, buckling (Zhu *et al*. 2017) bending (Wang *et al*. 2016), and

*Corresponding author, Ph.D.,
E-mail: febrahimy@eng.ikiu.ac.ir; febrahimy@gmail.com

ISSN: 2287-237X (Print), 2287-2388 (Online)

vibration (Fernández-Sáez and Zaera 2017) of Euler-Bernoulli nanobeams, and longitudinal vibration of nannorods (Zhu and Li 2017) have been investigated. In addition, on the basis of two-phase theory, the coupling between lateral and axial deflection caused by an attached mass on a nanosensor was studied by Naderi *et al*. (2020). Fakher and Hosseini-Hashemi (2020b) studied the exact solution for a beam modeled using two-phase elasticity as well as Timoshenko beam theory. Nonlinear vibration of nanobeam modeled using two-phase elasticity has been studied by Fakher and Hosseini-Hashemi (2020a). Additionally, Behdad *et al*. (2021) studied dynamic stability of beam modeled by Timoshenko beam theory and made of VFGP material by using two-phase elasticity. Fakher *et al*. (2020) investigated the effect of using size-dependent thermal load and elastic foundation on buckling and vibration of nanobeams.

To investigate the size-dependent characteristic of piezoelectric structures, a model on the basis of differential nonlocal theory was developed (Zhou and Wang 2002, Zhou *et al*. 2006, 2007). Hence, a large number of researches has been done using differential nonlocal model for piezoelectric material. For example, thermoelectric-mechanical nonlinear (Ke *et al*. 2012) and linear (Ke and Wang 2012) vibration of nanobeams modeled by Timoshenko beam theory was investigated. Buckling of the beams made of functionally graded piezoelectric material was studied through differential nonlocal and using higher-order shear deformable theory (Ebrahimi and Barati 2017). In addition, using differential nonlocal theory for piezoelectric materials and Mindlin plate, mechanical, thermal, and also electrical vibration of plates, Ke *et al*. (2015) studied through using DQ method. Moreover, recently, by using two-phase local/nonlocal theory as paradox-free, vibration, buckling, and energy harvesting of a nanobeam made of piezoelectric material was studied by Naderi *et al*. (2021). In this work, also, they studied the effect of capturing the size-dependency of piezoelectric load.

As previously stated, numerous researchers have published their findings on the vibration response, control, and energy harvesting of one, two, or more phases of composite beams, however, the investigation of vibration control and energy harvesting based on nonlocal elasticity on the substrate under blast loads requires additional research. Consequently, controlled vibration and energy harvesting are explored in the present study using two-phase nonlocal elasticity on a three-layered beam comprised of a nonpiezoelectric core and two piezoelectric layers on an elastic foundation subjected to a blast load. The governing equations and boundary conditions are deduced using the Hamilton principle. After deriving the governing equation from to-phase elasticity, the governing equation is solved using GDQM and the Newmark beta method. A reference article is used to validate both the formulation and the technique of the solution. It has been shown that a size-dependent elastic foundation may reduce the amplitude of vibrations. Additionally, a system that utilizes a nonpiezo-electric layer that is softer than piezoelectric layers may improve the system,s capacity to gather energy.

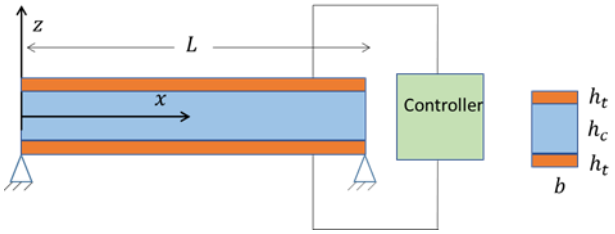

Fig. 1 Schematic of a three-layer beam including a core layer as well as two piezoelectric layers connected to a controller

2. Methodology

This part presents the equations of motion and associated boundary conditions of a two-phase Euler-Bernoulli nanobeam at the top and the bottom, where two piezo-electric layers are placed, presented in Fig. 1.

The Hamilton principle as a strong technique is used as follows in order to derive the governing equations and related boundary conditions of a bi-layered beam, involving a core layer and two piezoelectric layers resting on an elastic medium (Ma *et al*. 2022, Zhao *et al*. 2022, Hou *et al*. 2021, Huang *et al*. 2021b, c, Jiao *et al*. 2021, Liu *et al*. 2021c, Moradi *et al*. 2021, Xu *et al*. 2021, Dong *et al*. 2022, Luo *et al*. 2022, Michael *et al*. 2022, Wang *et al*. 2022b, Yang *et al*. 2022, Yu *et al*. 2022c).

$$\int_{t_1}^{t_2} \delta(\Pi - \Gamma)\, dt = 0 \tag{1}$$

In the obtained equation, Π, is the kinetic energy, and, Γ, is the strain energy of the composite beam. Displacements fields in the longitudinal and transverse direction, U_x, U_y, and U_z according to Euler-Bernoulli beam theory are defined as follows (Habibi *et al*. 2016, 2018a, b, 2019b, d, e, Ebrahimi *et al*. 2019a, Esmailpoor Hajilak *et al*. 2019, Pourjabari *et al*. 2019, Safarpour *et al*. 2019a):

$$\begin{aligned} u_x(x,z,t) &= u(x,t) - z\frac{\partial w(x,t)}{\partial x} \\ u_y(x,z,t) &= 0 \\ u_z(x,z,t) &= w(x,t) \end{aligned} \tag{2}$$

Also, related non-zero strain, ε_{xx}, are as follow, respectively.

$$\varepsilon_{xx} = -z\frac{\partial^2 w(x,t)}{\partial x^2} \tag{3}$$

where $w(x,t)$ is the lateral displacement of the neutral axis of the nanobeam. Based on the assumption of Wang (2002), the electrical potential of piezoelectric layers can be assumed as the following (Habibi *et al*. 2017, 2019a, c, Safarpour *et al*. 2018, 2019b, 2020, Alipour *et al*. 2020, Ebrahimi *et al*. 2020a, Ghazanfari *et al*. 2020, Chen *et al*. 2022).

$$\begin{aligned} &\Phi^t(x,z,t) \\ &= -\cos\left(\beta^t\left(z-\frac{h_c}{2}\right)\right)\phi^t(x,t) + \frac{2\left(z-\frac{h_c}{2}\right)V_0}{h_t}e^{i\Omega t} \end{aligned} \tag{4a}$$

$$\Phi^b(x,z,t) = -\cos\left(\beta^b\left(z+\frac{h_c}{2}\right)\right)\phi^b(x,t) \tag{4b}$$

where $\phi(x,t)$ is the variation of the electrical potential for the top and bottom layer respectively, V_0 is external voltage, $\beta^t=\pi/h_t$, and $\beta^b=\pi/h_b$. Now, using Eq. (4), the electrical field in transverse z-direction can be obtained as follows:

$$\begin{aligned} E_z^t &= -\frac{\partial\Phi}{\partial z} \\ &= -\beta^t \sin\left(\beta^t\left(z-\frac{h_c}{2}\right)\right)\phi^t(x,t) - \frac{2V_0}{h_t}e^{i\Omega t} \end{aligned} \tag{5a}$$

$$E_z^b = -\frac{\partial\Phi}{\partial z} = -\beta^b \sin\left(\beta^b\left(z+\frac{h_c}{2}\right)\right)\phi^b(x,t) \tag{5b}$$

Potential energy of a system including one core layer and two piezoelectric layers is written as follows (Ebrahimi *et al*. 2019b, c, Hashemi *et al*. 2019, Moayedi *et al*. 2019, 2020a, b, Mohammadgholiha *et al*. 2019, Mohammadi *et al*. 2019, Ebrahimi *et al*. 2020c, Habibi *et al*. 2020, Oyarhossein *et al*. 2020, Shariati *et al*. 2020a, b, Shokrgozar *et al*. 2020):

$$\begin{aligned} \Gamma = \frac{1}{2}\int_{A_c}\int_0^L (\sigma_{xx}\varepsilon_{xx})\,dxdA_c \\ + \frac{1}{2}\int_{A_p}\int_0^L (\sigma_{xx}\varepsilon_{xx} - D_z E_z)\,dxdA_p \end{aligned} \tag{6}$$

The axial stress relation for core layer as well as piezoelectric layers presented respectively (Fan *et al*. 2022, Wang *et al*. 2022a, Xia *et al*. 2022).

$$\sigma_{xx}^c = C_{11}\varepsilon_{xx} \tag{7a}$$

$$\sigma_{xx}^p = Q_{11}\varepsilon_{xx} - e_{31}E_z \tag{7b}$$

where C_{11} and Q_{11} are the elastic modulus, and e_{31} denote the piezoelectric constant. Also, the electrical displacement for piezoelectric layers can be obtained as following (Hashemi *et al*. 2019, Al-Furjan *et al*. 2020c, d, e, f, Bai *et al*. 2020, Cheshmeh *et al*. 2020, Li *et al*. 2020a, Lori *et al*. 2020, Najaafi *et al*. 2020, Shariati *et al*. 2020c, Xiong *et al*. 2020, Guo *et al*. 2021b, Liu *et al*. 2021a).

$$D_z = e_{31}\varepsilon_{xx} + \in_{33} E_z \tag{8}$$

In which $\in_{33}$ denotes dielectric constant. The potential energy of the system can be rewritten as follows:

$$\begin{aligned} \Gamma = \frac{1}{2}\int_{-h_c/2}^{h_c/2}\int_0^L \left(-\sigma_{xx}z\frac{\partial^2 w(x,t)}{\partial x^2}\right)dxdz \\ + \int_{h_c/2}^{h_c/2+h_t}\int_0^L \left(-\sigma_{xx}z\frac{\partial^2 w(x,t)}{\partial x^2}\right. \\ + D_z\left(\beta^t \sin\left(\beta^t\left(z-\frac{h_c}{2}\right)\right)\phi^t\right. \\ \left.\left. + \frac{2V_0}{h^t}e^{i\Omega t}\right)\right)dxdz + \\ \int_{-h_c/2-h_b}^{-h_c/2}\int_0^L \left(-\sigma_{xx}z\frac{\partial^2 w(x,t)}{\partial x^2}\right. \\ + D_z\left(\beta^b \sin\left(\beta^b\left(z\right.\right.\right. \\ \left.\left.\left. + \frac{h_c}{2}\right)\right)\phi^b(x,t)\right)\right)dxdz \end{aligned} \tag{9}$$

The bending moment, $M(x,t)$ can be written as

$$\begin{aligned} M(x,t) \\ = \int_{-h/2}^{h/2} z\sigma_{xx}^c dz + \int_{h_c/2}^{h_c/2+h_t} z\sigma_{xx}^p dz + \int_{-h_c/2-h_b}^{-h_c/2} z\sigma_{xx}^p dz \end{aligned} \tag{10}$$

By using the Eq. (9), and Eq. (10), the strain energy of beam can be re-written as follows:

$$\begin{aligned} \Gamma \\ = \int_0^L \left(\begin{array}{c} \left(\begin{array}{c} -\frac{1}{2}N(x,t)\left(\frac{\partial w(x,t)}{\partial x}\right)^2 \\ -M(x,t)\frac{\partial^2 w(x,t)}{\partial x^2} \end{array}\right) + \\ \int_{-h_c/2-h_b}^{-h_c/2}\left(\begin{array}{c} -\sigma_{xx}z\frac{\partial^2 w(x,t)}{\partial x^2} \\ +D_z\left(\beta^b \sin\left(\beta^b\left(z+\frac{h_c}{2}\right)\right)\phi^b(x,t)\right) \end{array}\right)dz + \\ \int_{h_c/2}^{h_c/2+h_t}\left(\begin{array}{c} -\sigma_{xx}z\frac{\partial^2 w(x,t)}{\partial x^2} \\ +D_z\left(\beta^t \sin\left(\beta^t\left(z-\frac{h_c}{2}\right)\right)\phi^t + \frac{2V_0}{h^t}e^{i\Omega t}\right) \end{array}\right)dz \end{array}\right)dx \end{aligned} \tag{11}$$

Having presented the potential energy, the kinetic energy of the system, Π, should be expressed as follows.:

$$\Pi = \frac{1}{2}\int_0^L m_1\left(\frac{\partial w(x,t)}{\partial t}\right)^2 dx \tag{12}$$

where

$$m_1 = \int_{-\frac{h}{2}}^{\frac{h}{2}}\rho^c dz + \int_{-h_t/2}^{h_t/2}\rho^p dz + \int_{-h_b/2}^{-h_b/2}\rho^p dz \tag{13}$$

where ρ^p and ρ^c denote the mass density for piezoelectric layers as well as core layer. Then, by substituting Eqs. (11) and (12) into Eq. (1), and setting the coefficients of $\delta\phi^t$, $\delta\phi^b$, and δw equal to zero and adding the transverse force of the elastic foundation $R(x,t)$, the equations of motion are acquired

$$\frac{\partial^2 M(x,t)}{\partial x^2} - m_1\frac{\partial^2 w(x,t)}{\partial t^2} + R(x,t) = 0 \tag{14a}$$

$$\begin{aligned} \Im^t(x,t) \\ = \int_{h_c/2}^{h_c/2+h_t} D_z\left(\beta^t \sin\left(\beta^t\left(z-\frac{h_c}{2}\right)\right)\phi^t + \frac{2V_0}{h^t}e^{i\Omega t}\right)dz \\ = 0 \end{aligned} \tag{14b}$$

$$\begin{aligned} \Im^b(x,t) \\ = \int_{-h_c/2-h_b}^{-h_c/2} D_z\left(\beta^b \sin\left(\beta^b\left(z+\frac{h_c}{2}\right)\right)\phi^b(x,t)\right)dz = 0 \end{aligned} \tag{14c}$$

Additionally, the relations associated to various boundary conditions can be expressed as follows:

Clamped:

$$w(x,t)=0 \quad \text{And} \quad \frac{\partial w(x,t)}{\partial x}=0 \tag{15a}$$

Free:

$$M(x,t)=0 \quad \text{And} \quad \frac{\partial M(x,t)}{\partial x}=0 \tag{15b}$$

Simply supported:

$$w(x,t)=0 \quad \text{And} \quad M(x,t)=0 \tag{15c}$$

2.1 Two- phase elasticity

Stress-strain relation Based on two-phase elasticity for a 1-D isotropic structure is as follows:

$$t(x)=\zeta\bar{C}:\varepsilon(x)+(1-\zeta)\int_{\bar{V}}\alpha(x,\bar{x},\kappa)\bar{C}:\varepsilon(\bar{x})d\bar{V} \tag{16a}$$

$$\alpha(x,\bar{x},k)=\frac{1}{2\kappa}e^{-\frac{|x-\bar{x}|}{\kappa}} \tag{16b}$$

where $t(x)$, $\varepsilon(x)$, $\alpha(x,\bar{x},\kappa),\bar{C}$, ζ, $\bar{V}$, and κ denote two-phase stress, strain tensor, Kernel function, elasticity tensor, local phase fraction, volume of all domain, and nonlocal factor respectively. The differential form, Eq. (17b), of the integral equation, Eq. (17a), has been introduced by Polyanin and Manzhirov (2008), and it was shown that if the equal differential form is used, the constitutive boundary conditions (CBC), Eqs. (17c) and (17d), must be satisfied.

$$y(x)+C\int_a^b e^{\mu|x-\bar{x}|}y(\bar{x})d\bar{x}=g(x) \tag{17a}$$

$$y''(x)+\mu(2C-\mu)y(x)=g''(x)-\mu^2 g(x) \tag{17b}$$

$$y'(a)+\mu y(a)=g'(a)+\mu g(a) \tag{17c}$$

$$y'(b)-\mu y(b)=g'(b)-\mu g(b) \tag{17d}$$

where, C, and, μ, are constant coefficients.

2.2 Two-phase bending moment

With the aid of two-phase elasticity, the local/nonlocal normal stress of a system including a core layer and two piezoelectric layers is attained, using Eq. (7) and Eq. (16)

$$\begin{aligned}&\sigma=\zeta(C_{11}\varepsilon_{xx}+Q_{11}\varepsilon_{xx}-e_{31}E_z)\\&+\frac{(1-\zeta)}{2\kappa}\int_L e^{-\frac{|x-\bar{x}|}{\kappa}}(C_{11}\varepsilon_{\bar{x}\bar{x}}+Q_{11}\varepsilon_{\bar{x}\bar{x}}-e_{31}E_z)d\bar{x}\end{aligned} \tag{18}$$

Now, by using Eq. (18) and Eq. (10), the two-phase bending moment for the given system can be written in the basic integral form

$$\begin{aligned}&M(x,t)\\&=\zeta\left(-D_{11}\frac{\partial^2 w(x,t)}{\partial x^2}+F^t\phi^t(x,t)+F^b\phi^b(x,t)\right)\\&+\frac{(1-\zeta)}{2\kappa}\int_0^L e^{-\frac{|x-\bar{x}|}{\kappa}}\left(-D_{11}\frac{\partial^2 w(x,t)}{\partial x^2}+F^t\phi^t(x,t)\right.\\&\left.+F^b\phi^b(x,t)\right)d\bar{x}\end{aligned} \tag{19}$$

where

$$D_{11}=\int_{A_c}C_{11}z^2dA+\int_{A_p}Q_{11}z^2dA \tag{20a}$$

$$F^b=b\int_{-h_c/2-h_b}^{-h_c/2}e_{31}\beta^b sin\left(\beta^b\left(z+\frac{h_c}{2}\right)\right)zdz \tag{20b}$$

$$F^t=b\int_{h_c/2}^{h_c/2+h_t}e_{31}\beta^t sin\left(\beta^t\left(z-\frac{h_c}{2}\right)\right)zdz \tag{20c}$$

With considering Eq. (17a) and Eq. (17b), and also using Eq. (18) as well as the first part of Eq. (14), the differential form of two-phase bending moment is obtained.

$$\begin{aligned}&M(x,t)=m_1\kappa^2\frac{\partial^2 w(x,t)}{\partial t^2}+F^t\phi^t(x,t)+F^b\phi^b(x,t)\\&+(-D_{11})\frac{\partial^2 w(x,t)}{\partial x^2}-F^t\kappa^2\zeta\frac{\partial^2\phi^t(x,t)}{\partial x^2}\\&-F^b\kappa^2\zeta\frac{\partial^2\phi^b(x,t)}{\partial x^2}+D_{11}\kappa^2\zeta\frac{\partial^4 w(x,t)}{\partial x^4}-\kappa^2R(x,t)\end{aligned} \tag{21}$$

Also, by employing the first part of Eq. (14) and Eq. (21), the differential governing equation of the piezoelectric nanobeam can be derived in the frame work of two-phase elasticity as follows:

$$\begin{aligned}&D_{11}\kappa^2\zeta\frac{\partial^6 w(x,t)}{\partial x^6}+(-D_{11})\frac{\partial^4 w(x,t)}{\partial x^4}\\&+\left(m_1\kappa^2\frac{\partial^2}{\partial t^2}\right)\frac{\partial^2 w(x,t)}{\partial x^2}-F^t\kappa^2\zeta\frac{\partial^4\phi^t(x,t)}{\partial x^4}\\&-F^b\kappa^2\zeta\frac{\partial^4\phi^b(x,t)}{\partial x^4}+F^t\frac{\partial^2\phi^t(x,t)}{\partial x^2}+F^b\frac{\partial^2\phi^b(x,t)}{\partial x^2}\\&-m_1\frac{\partial^2 w(x,t)}{\partial t^2}-\kappa^2\frac{\partial^2 R(x,t)}{\partial x^2}+R(x,t)=0\end{aligned} \tag{22}$$

Lastly, by utilizing Eqs. (17) and Eq. (19), the two CBCs related to the bending boundary moment at left side of beam (x=0) is obtained as follows:

$$\begin{aligned}&M(0,t)=\frac{F^t(1-\zeta)}{\kappa\zeta}\phi^t(x,t)+\frac{F^t(\zeta-1)}{\zeta}\frac{\partial\phi^t(x,t)}{\partial x}\\&-F^t\kappa\frac{\partial^2\phi^t(x,t)}{\partial x^2}+F^t\kappa^2\frac{\partial^3\phi^t(x,t)}{\partial x^3}\\&\frac{F^b(1-\zeta)}{\kappa\zeta}\phi^b(x,t)+\frac{F^b(\zeta-1)}{\zeta}\frac{\partial\phi^b(x,t)}{\partial x}\\&-F^b\kappa\frac{\partial^2\phi^b(x,t)}{\partial x^2}+F^b\kappa^2\frac{\partial^3\phi^b(x,t)}{\partial x^3}\\&+\frac{m_1\kappa}{\zeta}\frac{\partial^2 w(x,t)}{\partial t^2}-\frac{m_1\kappa^2}{\zeta}\frac{\partial^3 w(x,t)}{\partial t^2\partial x}\\&+\frac{(-D_{11}+D_{11}\zeta)}{\kappa\zeta}\frac{\partial^2 w(x,t)}{\partial x^2}\\&+\frac{(D_{11}-D_{11}\zeta)}{\zeta}\frac{\partial^3 w(x,t)}{\partial x^3}+D_{11}\kappa\frac{\partial^4 w(x,t)}{\partial x^4}\end{aligned} \tag{23a}$$

$$-D_{11}\kappa^2\frac{\partial^5 w(x,t)}{\partial x^5}+\frac{\kappa^2}{\zeta}\frac{\partial R(x,t)}{\partial x}-\frac{\kappa}{\zeta}R(x,t)=0$$

and the bending boundary moment at dight side of beam (x=L) is obtained as follows:

$$\begin{aligned}
&M(L,t)=\frac{F^t(\zeta-1)}{\kappa\zeta}\phi^t(x,t)+\frac{F^t(\zeta-1)}{\zeta}\frac{\partial\phi^t(x,t)}{\partial x}\\
&+F^t\kappa\frac{\partial^2\phi^t(x,t)}{\partial x^2}+F^t\kappa^2\frac{\partial^3\phi^t(x,t)}{\partial x^3}\\
&\frac{F^b(\zeta-1)}{\kappa\zeta}\phi^b(x,t)+\frac{F^b(\zeta-1)}{\zeta}\frac{\partial\phi^b(x,t)}{\partial x}\\
&+F^b\kappa\frac{\partial^2\phi^b(x,t)}{\partial x^2}+F^b\kappa^2\frac{\partial^3\phi^b(x,t)}{\partial x^3}\\
&-\frac{m_1\kappa}{\zeta}\frac{\partial^2 w(x,t)}{\partial t^2}-\frac{m_1\kappa^2}{\zeta}\frac{\partial^3 w(x,t)}{\partial t^2\partial x}\\
&+\frac{(D_{11}-D_{11}\zeta)}{\kappa\zeta}\frac{\partial^2 w(x,t)}{\partial x^2}+\frac{\kappa^2}{\zeta}\frac{\partial R(x,t)}{\partial x}\\
&+\frac{(D_{11}-A_{11}\zeta)}{\zeta}\frac{\partial^3 w(x,t)}{\partial x^3}-D_{11}\kappa\frac{\partial^4 w(x,t)}{\partial x^4}\\
&-D_{11}\kappa^2\frac{\partial^5 w(x,t)}{\partial x^5}+\frac{\kappa}{\zeta}R(x,t)=0
\end{aligned}\tag{23b}$$

2.3 Two-phase electric displacement

To apply the nonlocality of the electric displacement, which has been ever considered by the differential nonlocal of Zhou and Wang (2002), using Eq. (8) and Eq. (16), the relation corresponding to the two-phase electric displacement is expressed as follows:

$$\begin{aligned}
&D_z=\zeta(e_{31}\varepsilon_{xx}+\in_{33}E_z)\\
&+\frac{(1-\zeta)}{2\kappa}\int_L e^{-\frac{|x-\bar{x}|}{\kappa}}(e_{31}\varepsilon_{xx}+\in_{33}E_z)d\bar{x}
\end{aligned}\tag{24}$$

Then, by integration of $D_z\beta sin(\beta z)$ over the surface of each layer, *A*, gives

$$\begin{aligned}
&\Im^t(x,t)=\int_A D_z\beta^t sin\left(\beta^t\left(z-\frac{h_c}{2}\right)\right)dA\\
&=\zeta\left(F^t\frac{\partial^2 w(x,t)}{\partial x^2}+X^t\phi^t(x,t)\right)\\
&+\frac{(1-\zeta)}{2\kappa}\int_0^L e^{-\frac{|x-\bar{x}|}{\kappa}}\left(F^t\frac{\partial^2 w(\bar{x},t)}{\partial\bar{x}^2}+X^t\phi^b(\bar{x},t)\right)d\bar{x}
\end{aligned}\tag{25a}$$

$$\begin{aligned}
&\Im^b(x,t)=\int_A D_z\beta^b sin\left(\beta^b\left(z+\frac{h_c}{2}\right)\right)dA\\
&=\zeta\left(F^b\frac{\partial^2 w(x,t)}{\partial x^2}+X^b\phi^b(x,t)\right)\\
&+\frac{(1-\zeta)}{2\kappa}\int_0^L e^{-\frac{|x-\bar{x}|}{\kappa}}\left(F^b\frac{\partial^2 w(\bar{x},t)}{\partial\bar{x}^2}+X^b\phi^b(\bar{x},t)\right)d\bar{x}
\end{aligned}\tag{25b}$$

In which

$$X^t=b\int_{h_c/2}^{h_c/2+h_t}\eta\left(\beta^t sin\left(\beta^t\left(z-\frac{h_c}{2}\right)\right)\right)^2dz\tag{26a}$$

$$X^b=b\int_{-h_c/2-h_b}^{-h_c/2}\eta\left(\beta^b sin\left(\beta^b\left(z+\frac{h_c}{2}\right)\right)\right)^2dz\tag{26b}$$

Thus, the two-phase differential equation governed on the electric displacement can be produced using Eq. (25) and the second part Eq. (14) as follows:

$$\begin{aligned}
&-F^t\kappa^2\zeta\frac{\partial^4 w(x,t)}{\partial x^4}+F^t\frac{\partial^2 w(x,t)}{\partial x^2}-\kappa^2X^t\zeta\frac{\partial^2\phi^t(x,t)}{\partial x^2}\\
&+X^t\phi^t(x,t)\\
&=-\kappa^2\frac{\partial^2\Im^t(x,t)}{\partial x^2}+\Im^t(x,t)\Im^t(x,t)\\
&=\frac{\partial\Im^t(x,t)}{\partial x}=\frac{\partial^2\Im^t(x,t)}{\partial x^2}
\end{aligned}\tag{27a}$$

$$\begin{aligned}
&-F^b\kappa^2\zeta\frac{\partial^4 w(x,t)}{\partial x^4}+F^b\frac{\partial^2 w(x,t)}{\partial x^2}\\
&-\kappa^2X^b\zeta\frac{\partial^2\phi^b(x,t)}{\partial x^2}+X^b\phi^b(x,t)\\
&=-\kappa^2\frac{\partial^2\Im^t(x,t)}{\partial x^2}+\Im^t(x,t)\Im^b(x,t)\\
&=\frac{\partial\Im^b(x,t)}{\partial x}=\frac{\partial^2\Im^b(x,t)}{\partial x^2}
\end{aligned}\tag{27b}$$

Similarly, the CBCs for electric displacement are obtained by utilizing Eq. (25) and Eqs. (17), that the boundary conditions are obtain as follows:

$$-\frac{X^t}{\kappa}\phi^t(x,t)+X^t\frac{\partial\phi^t(x,t)}{\partial x}-\frac{F^t}{\kappa}\frac{\partial^2 w(x,t)}{\partial x^2}+F^t\frac{\partial^3 w(x,t)}{\partial x^3}=0\quad\text{at x=0}\tag{28a}$$

$$-\frac{X^b}{\kappa}\phi^b(x,t)+X^n\frac{\partial\phi^n(x,t)}{\partial x}-\frac{F^n}{\kappa}\frac{\partial^2 w(x,t)}{\partial x^2}+F^n\frac{\partial^3 w(x,t)}{\partial x^3}=0\quad\text{at x=0}\tag{28b}$$

$$\frac{X^t}{\kappa}\phi^t(x,t)+X^t\frac{\partial\phi^t(x,t)}{\partial x}+\frac{F^t}{\kappa}\frac{\partial^2 w(x,t)}{\partial x^2}+F^t\frac{\partial^3 w(x,t)}{\partial x^3}=0\quad\text{at x=0}\tag{28c}$$

$$\frac{X^b}{\kappa}\phi^b(x,t)+X^b\frac{\partial\phi^b(x,t)}{\partial x}+\frac{F^b}{\kappa}\frac{\partial^2 w(x,t)}{\partial x^2}+F^b\frac{\partial^3 w(x,t)}{\partial x^3}=0\quad\text{at x=0}\tag{28d}$$

2.4 Two-phase elastic medium

In this section, the two-phase local nonlocal force for elastic force is obtained. Accordingly, since the classic force for the elastic medium can be obtained from "$R^{classic}=-k_f w(x,t)$", two-phase form of this force can be written as follows:

$$R(x,t)=-\zeta k_f w(x,t)-\frac{(1-\zeta)}{2\kappa}\int_L e^{-\frac{|x-\bar{x}|}{\kappa}}k_f w(\bar{x},t)d\bar{x}\tag{29}$$

Thus, two-phase differential equation for elastic

medium force can be produced using Eq. (29) and the second part Eq. (14) according to following equation:

$$\kappa^2 \frac{\partial^2 R(x,t)}{\partial x^2} - R(x,t) + \zeta \kappa^2 k_f \frac{\partial^2 w(x,t)}{\partial x^2} - k_f w(x,t) = 0 \quad (30)$$

Similarly, the CBCs for elastic medium force are obtained by utilizing Eq. (29) and Eqs. (17) as follows:

$$\kappa \frac{\partial R(x,t)}{\partial x} - R(x,t) + \zeta \kappa k_f \frac{\partial w(x,t)}{\partial x} - \zeta k_f w(x,t) = 0 \quad \text{at } x = L \quad (31a)$$

$$\kappa \frac{\partial R(x,t)}{\partial x} + R(x,t) + \zeta \kappa k_f \frac{\partial w(x,t)}{\partial x} + \zeta k_f w(x,t) = 0 \quad \text{at } x = 0 \quad (31b)$$

In the following, the nondimensional parameters are defined as follows:

$$\begin{aligned} &\bar{x} = \frac{x}{L}, \bar{w} = \frac{w}{h_{tot}}, \bar{\phi}^t = \frac{\phi^t}{\phi_0^t}, \bar{\phi}^b = \frac{\phi^b}{\phi_0^b}, \\ &\phi_0^b = \sqrt{\frac{A_{11}}{X^b}}, \phi_0^t = \sqrt{\frac{A_{11}}{X^t}}, \bar{\kappa} = \frac{\kappa}{L}, \bar{R} = \frac{R D_{11}}{A_{11} L^2} \\ &\bar{F}^t = \frac{F^t \phi_0^t}{A_{11} h_{tot}}, \bar{F}^b = \frac{F^b \phi_0^b}{A_{11} h_{tot}}, \bar{D}_{11} = \frac{D_{11}}{L^2 A_{11}}, \\ &X^t = \frac{X^t (\phi_0^t)^2 L^2}{{h_{tot}}^2 A_{11}}, X^b = \frac{X^b (\phi_0^b)^2 L^2}{{h_{tot}}^2 A_{11}} \end{aligned} \quad (32)$$

The nondimensional form of Eqs. (22), (27), and (28) are reform to following:

$$\begin{aligned} &\bar{D}_{11} \bar{\kappa}^2 \zeta \frac{\partial^6 \bar{w}(\bar{x},\tau)}{\partial \bar{x}^6} + (-\bar{D}_{11}) \frac{\partial^4 \bar{w}(\bar{x},\tau)}{\partial \bar{x}^4} \\ &+ \left(\bar{\kappa}^2 \frac{\partial^2}{\partial \tau^2} \right) \frac{\partial^2 \bar{w}(\bar{x},\tau)}{\partial \bar{x}^2} - \bar{F}^t \bar{\kappa}^2 \zeta \frac{\partial^4 \bar{\phi}^t(\bar{x},\tau)}{\partial \bar{x}^4} \\ &- \bar{F}^b \bar{\kappa}^2 \zeta \frac{\partial^4 \bar{\phi}^b(\bar{x},\tau)}{\partial \bar{x}^4} + \bar{F}^t \frac{\partial^2 \bar{\phi}^t(\bar{x},\tau)}{\partial \bar{x}^2} + \bar{F}^b \frac{\partial^2 \bar{\phi}^b(\bar{x},\tau)}{\partial \bar{x}^2} \\ &- \frac{\partial^2 \bar{w}(\bar{x},\tau)}{\partial \tau^2} - \bar{\kappa}^2 \frac{\partial^2 \bar{R}(\bar{x},\tau)}{\partial \bar{x}^2} + \bar{R}(\bar{x},\tau) = 0 \end{aligned} \quad (33a)$$

$$\begin{aligned} &-\bar{F}^t \bar{\kappa}^2 \zeta \frac{\partial^4 \bar{w}(\bar{x},\tau)}{\partial \bar{x}^4} + \bar{F}^t \frac{\partial^2 \bar{w}(\bar{x},\tau)}{\partial \bar{x}^2} \\ &-\bar{\kappa}^2 \bar{X}^t \zeta \frac{\partial^2 \bar{\phi}^t(\bar{x},\tau)}{\partial \bar{x}^2} + \bar{X}^t \bar{\phi}^t(\bar{x},\tau) = 0 \end{aligned} \quad (33b)$$

$$\begin{aligned} &-\bar{F}^b \bar{\kappa}^2 \zeta \frac{\partial^4 \bar{w}(\bar{x},\tau)}{\partial \bar{x}^4} + \bar{F}^b \frac{\partial^2 \bar{w}(\bar{x},\tau)}{\partial \bar{x}^2} \\ &-\bar{\kappa}^2 \bar{X}^b \zeta \frac{\partial^2 \bar{\phi}^b(\bar{x},\tau)}{\partial \bar{x}^2} + \bar{X}^b \bar{\phi}^b(\bar{x},\tau) = 0 \end{aligned} \quad (33c)$$

$$\begin{aligned} &\bar{\kappa}^2 \frac{\partial^2 \bar{R}(\bar{x},\tau)}{\partial \bar{x}^2} - \bar{R}(\bar{x},\tau) + \zeta \bar{\kappa}^2 k_f \frac{\partial^2 \bar{w}(\bar{x},\tau)}{\partial \bar{x}^2} \\ &-k_f \bar{w}(\bar{x},\tau) = 0 \end{aligned} \quad (33d)$$

And the boundary conditions are reformed as follows:

$$\begin{aligned} &\frac{\bar{F}^\tau (1-\zeta)}{\bar{\kappa}\zeta} \bar{\phi}^\tau(\bar{x},\tau) + \frac{\bar{F}^\tau (\zeta-1)}{\zeta} \frac{\partial \bar{\phi}^\tau(\bar{x},\tau)}{\partial \bar{x}} \\ &-\bar{F}^\tau \bar{\kappa} \frac{\partial^2 \bar{\phi}^\tau(\bar{x},\tau)}{\partial \bar{x}^2} + \bar{F}^\tau \bar{\kappa}^2 \frac{\partial^3 \bar{\phi}^\tau(\bar{x},\tau)}{\partial \bar{x}^3} \end{aligned} \quad \text{at } \bar{x}=0 \quad (34a)$$

$$\begin{aligned} &\frac{\bar{F}^b (1-\zeta)}{\bar{\kappa}\zeta} \bar{\phi}^b(\bar{x},\tau) + \frac{\bar{F}^b (\zeta-1)}{\zeta} \frac{\partial \bar{\phi}^b(\bar{x},\tau)}{\partial \bar{x}} \\ &-\bar{F}^b \bar{\kappa} \frac{\partial^2 \bar{\phi}^b(\bar{x},\tau)}{\partial \bar{x}^2} + \bar{F}^b \bar{\kappa}^2 \frac{\partial^3 \bar{\phi}^b(\bar{x},\tau)}{\partial \bar{x}^3} \\ &+ \frac{\bar{\kappa}}{\zeta} \frac{\partial^2 \bar{w}(\bar{x},\tau)}{\partial \tau^2} - \frac{\bar{\kappa}^2}{\zeta} \frac{\partial^3 \bar{w}(\bar{x},\tau)}{\partial \tau^2 \partial \bar{x}} \\ &+ \frac{(-\bar{D}_{11} + \bar{D}_{11}\zeta)}{\bar{\kappa}\zeta} \frac{\partial^2 \bar{w}(\bar{x},\tau)}{\partial \bar{x}^2} + \frac{\bar{\kappa}^2}{\zeta} \frac{\partial \bar{R}(\bar{x},\tau)}{\partial \bar{x}} \\ &+ \frac{(\bar{D}_{11} - \bar{D}_{11}\zeta)}{\zeta} \frac{\partial^3 \bar{w}(\bar{x},\tau)}{\partial \bar{x}^3} + \bar{D}_{11} \bar{\kappa} \frac{\partial^4 \bar{w}(\bar{x},\tau)}{\partial \bar{x}^4} \\ &-\bar{D}_{11} \bar{\kappa}^2 \frac{\partial^5 \bar{w}(\bar{x},\tau)}{\partial \bar{x}^5} - \frac{\bar{\kappa}}{\zeta} \bar{R}(\bar{x},\tau) = 0 \end{aligned}$$

$$\begin{aligned} &-\frac{\bar{X}^t}{\bar{\kappa}} \bar{\phi}^t(\bar{x},\tau) + \bar{X}^t \frac{\partial \bar{\phi}^t(\bar{x},\tau)}{\partial \bar{x}} - \frac{\bar{F}^t}{\bar{\kappa}} \frac{\partial^2 \bar{w}(\bar{x},\tau)}{\partial \bar{x}^2} \\ &+ \bar{F}^t \frac{\partial^3 \bar{w}(\bar{x},\tau)}{\partial \bar{x}^3} = 0 \end{aligned} \quad \text{at } \bar{x}=0 \quad (34b)$$

$$\begin{aligned} &-\frac{\bar{X}^b}{\bar{\kappa}} \bar{\phi}^b(\bar{x},\tau) + \bar{X}^b \frac{\partial \bar{\phi}^b(\bar{x},\tau)}{\partial \bar{x}} - \frac{\bar{F}^b}{\bar{\kappa}} \frac{\partial^2 \bar{w}(\bar{x},\tau)}{\partial \bar{x}^2} \\ &+ \bar{F}^b \frac{\partial^3 \bar{w}(\bar{x},\tau)}{\partial \bar{x}^3} = 0 \end{aligned} \quad \text{at } \bar{x}=0 \quad (34c)$$

$$\begin{aligned} &\bar{\kappa} \frac{\partial \bar{R}(\bar{x},\tau)}{\partial x} - \bar{R}(\bar{x},\tau) + \zeta \bar{\kappa} k_f \frac{\partial \bar{w}(\bar{x},\tau)}{\partial x} - \zeta k_f \bar{w}(\bar{x},\tau) \\ &= 0 \; at \; \bar{x} = 0 \end{aligned} \quad \text{at } \bar{x}=0 \quad (34d)$$

$$\begin{aligned} &\frac{\bar{F}^t (\zeta-1)}{\bar{\kappa}\zeta} \bar{\phi}^\tau(\bar{x},\tau) + \frac{\bar{F}^t (\zeta-1)}{\zeta} \frac{\partial \bar{\phi}^t(\bar{x},\tau)}{\partial \bar{x}} \\ &+\bar{F}^t \bar{\kappa} \frac{\partial^2 \bar{\phi}^t(\bar{x},\tau)}{\partial \bar{x}^2} + \bar{F}^t \bar{\kappa}^2 \frac{\partial^3 \bar{\phi}^t(\bar{x},\tau)}{\partial \bar{x}^3} \\ &\frac{\bar{F}^b (\zeta-1)}{\bar{\kappa}\zeta} \bar{\phi}^b(\bar{x},\tau) + \frac{\bar{F}^b (\zeta-1)}{\zeta} \frac{\partial \bar{\phi}^b(\bar{x},\tau)}{\partial \bar{x}} \\ &+\bar{F}^b \bar{\kappa} \frac{\partial^2 \bar{\phi}^b(\bar{x},\tau)}{\partial \bar{x}^2} + \bar{F}^b \bar{\kappa}^2 \frac{\partial^3 \bar{\phi}^b(\bar{x},\tau)}{\partial \bar{x}^3} \\ &-\frac{\bar{\kappa}}{\zeta} \frac{\partial^2 \bar{w}(\bar{x},\tau)}{\partial \tau^2} - \frac{\bar{\kappa}^2}{\zeta} \frac{\partial^3 \bar{w}(\bar{x},\tau)}{\partial \tau^2 \partial \bar{x}} \\ &+ \frac{(\bar{D}_{11} - \bar{D}_{11}\zeta)}{\bar{\kappa}\zeta} \frac{\partial^2 \bar{w}(\bar{x},\tau)}{\partial \bar{x}^2} + \frac{\bar{\kappa}^2}{\zeta} \frac{\partial \bar{R}(\bar{x},\tau)}{\partial \bar{x}} \\ &+ + \frac{(\bar{D}_{11} - A_{11}\zeta)}{\zeta} \frac{\partial^3 \bar{w}(\bar{x},\tau)}{\partial \bar{x}^3} - \bar{D}_{11} \bar{\kappa} \frac{\partial^4 \bar{w}(\bar{x},\tau)}{\partial \bar{x}^4} \\ &-\bar{D}_{11} \bar{\kappa}^2 \frac{\partial^5 \bar{w}(\bar{x},\tau)}{\partial \bar{x}^5} + \frac{\bar{\kappa}}{\zeta} \bar{R}(\bar{x},\tau) = 0 \end{aligned} \quad \text{at } \bar{x}=L \quad (34e)$$

$$\begin{aligned} &\frac{\bar{X}^t}{\bar{\kappa}} \bar{\phi}^t(\bar{x},\tau) + \bar{X}^t \frac{\partial \bar{\phi}^t(\bar{x},\tau)}{\partial \bar{x}} + \frac{\bar{F}^t}{\bar{\kappa}} \frac{\partial^2 \bar{w}(\bar{x},\tau)}{\partial \bar{x}^2} \\ &+ \bar{F}^t \frac{\partial^3 \bar{w}(\bar{x},\tau)}{\partial \bar{x}^3} = 0 \end{aligned} \quad \text{at } \bar{x}=L \quad (34f)$$

$$\begin{aligned} &\frac{\bar{X}^b}{\bar{\kappa}} \bar{\phi}^b(\bar{x},\tau) + \bar{X}^b \frac{\partial \bar{\phi}^b(\bar{x},\tau)}{\partial \bar{x}} + \frac{\bar{F}^b}{\bar{\kappa}} \frac{\partial^2 \bar{w}(\bar{x},\tau)}{\partial \bar{x}^2} \\ &+ \bar{F}^b \frac{\partial^3 \bar{w}(\bar{x},\tau)}{\partial \bar{x}^3} = 0 \end{aligned} \quad \text{at } \bar{x}=L \quad (34g)$$

$$\begin{aligned} &\bar{\kappa} \frac{\partial \bar{R}(\bar{x},\tau)}{\partial x} + \bar{R}(\bar{x},\tau) + \zeta \bar{\kappa} k_f \frac{\partial \bar{w}(\bar{x},\tau)}{\partial x} + \zeta k_f \bar{w}(\bar{x},\tau) \\ &= 0 \end{aligned} \quad \text{at } \bar{x}=L \quad (34h)$$

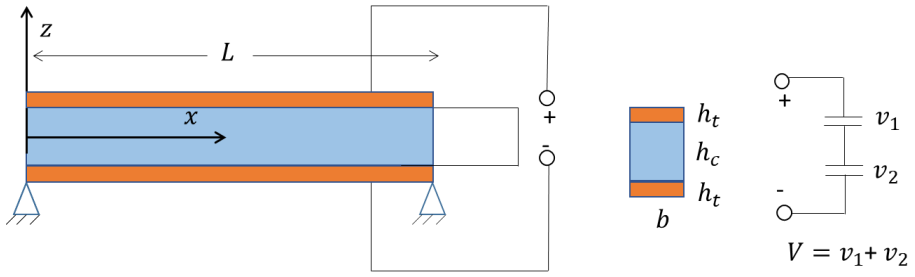

Fig. 2 Schematic of a three-layer beam including a core layer as well as two piezoelectric layers used as energy harvester

And nondimensional bending moment is represented as follows:

$$\bar{M}(\bar{x},\tau) = \bar{\kappa}^2 \frac{\partial^2 \bar{w}(\bar{x},\tau)}{\partial \tau^2} + \bar{F}^t \bar{\phi}^t(\bar{x},\tau) + \bar{F}^b \bar{\phi}^b(\bar{x},\tau) - (\bar{D}_{11}) \frac{\partial^2 \bar{w}(\bar{x},\tau)}{\partial \bar{x}^2} - \bar{F}^t \bar{\kappa}^2 \zeta \frac{\partial^2 \bar{\phi}^t(\bar{x},\tau)}{\partial \bar{x}^2} - \bar{F}^b \bar{\kappa}^2 \zeta \frac{\partial^2 \bar{\phi}^b(\bar{x},\tau)}{\partial \bar{x}^2} + \bar{D}_{11} \bar{\kappa}^2 \zeta \frac{\partial^4 \bar{w}(\bar{x},\tau)}{\partial \bar{x}^4} - \bar{\kappa}^2 \bar{R}(\bar{x},\tau) \quad (35)$$

3. Energy harvesting

In the present section, the electric potential generated by the system is equal to the total potential produced (Zhang *et al*. 2016, Wang *et al*. 2018, Jiang *et al*. 2021, Wu *et al*. 2022, Yan *et al*. 2022, Zhou *et al*. 2022) by the upper and lower piezoelectric layers, since the layers are linked together as shown in Fig. 2 to get the result for energy harvesting analysis.

3.1 Shockwave force

The force utilized in this research is a shockwave generated by a blast load, as described by Nguyen *et al*. (2017), and is given as follows:

$$F = P_{S0}\left[1 - \frac{t}{t_0}\right] exp\left(\frac{-at}{t_0}\right) \quad (36)$$

where and denote maximum static pressure as well as positive phase time which can be expressed as

$$P_{S0} = P0 \frac{808\left(1 + \left(\frac{Z}{4.5}\right)^2\right)}{1 + \left(\frac{Z}{0.048}\right)^2 \sqrt{1 + \left(\frac{Z}{1.35}\right)^2}} \quad (37a)$$

$$t_0 = \tilde{W}^{1/3} \frac{980\left(1 + \left(\frac{Z}{0.54}\right)^{10}\right)}{\left(1 + \left(\frac{Z}{0.02}\right)^3\right)\left(1 + \left(\frac{Z}{0.74}\right)^6\right)\sqrt{1 + \left(\frac{Z}{6.9}\right)^2}} ms \quad (37b)$$

In which, P_0, is atmosphere pressure and following constants are defined as follows:

$$Z = \frac{\tilde{R}}{\tilde{W}^{0.33}} \quad (38a)$$

$$a = 1.5Z^{-0.38} \quad (38b)$$

where, $\tilde{R}$ and $\tilde{W}$ are distance to of blast to the center of the beam and explosive material mass.

3.2 MHCD material formulation

The effective properties of MHCD which is based on Halpin-Tsai model is proposed as follow (Adamian *et al*. 2020, Al-Furjan *et al*. 2020a, b, Li *et al*. 2020b, Liu *et al*. 2020b, 2021b, Zare *et al*. 2020, Dai *et al*. 2021b, Habibi *et al*. 2021, He *et al*. 2021, Huang *et al*. 2021a, Zhang *et al*. 2021).

$$E = V_{NCM} E^{NCM} + V_F E_{11}^F \quad (39a)$$

$$\rho = V_{NCM} \rho^{NCM} + V_F \rho^F \quad (39b)$$

$$\nu = V_{NCM} \nu^{NCM} + V_F \nu^F \quad (39c)$$

The index *F* and *NCM* denotes to fiber and nanocomposite matrix. Also, the proportion of fiber and nanocomposites are

$$V_{NCM} + V_F = 1 \quad (40)$$

The Young's Modulus of nanocomposites can be obtained using the following formulations.

$$E^{NCM} = E^M \left(\left(\frac{3 + 6\left(\frac{l^{CNT}}{d^{CNT}}\right)\beta_{dl} V_{CNT}}{8 - 8\beta_{dl} V_{CNT}} \right) + \left(\frac{5 + 10\beta_{dd} V_{CNT}}{8 - 8\beta_{dd} V_{CNT}} \right) \right) \quad (41)$$

In which

$$\beta_{dd} = \frac{\left(\frac{E_{11}^{CNT}}{E^M}\right)}{\left(\frac{E_{11}^{CNT}}{E^M}\right) + \left(\frac{d^{CNT}}{2t^{CNT}}\right)} - \frac{\left(\frac{d^{CNT}}{4t^{CNT}}\right)}{\left(\frac{E_{11}^{CNT}}{E^M}\right) + \left(\frac{d^{CNT}}{2t^{CNT}}\right)} \quad (42a)$$

$$\beta_{dl} = \frac{\left(\frac{E_{11}^{CNT}}{E^M}\right)}{\left(\frac{E_{11}^{CNT}}{E^M}\right) + \left(\frac{l^{CNT}}{2t^{CNT}}\right)} - \frac{\left(\frac{d^{CNT}}{4t^{CNT}}\right)}{\left(\frac{E_{11}^{CNT}}{E^M}\right) + \left(\frac{l^{CNT}}{2t^{CNT}}\right)} \quad (42b)$$

$$V_{CNT}^* = \frac{W_{CNT}}{W_{CNT} + \left(\frac{\rho^{CNT}}{\rho^M}\right)(1 - W_{CNT})} \quad (42c)$$

$$V_{CNT} = 4V_{CNT}^{*}\frac{|\xi_j|}{h_c}FG - X \tag{42d}$$

$$V_{CNT} = V_{CNT}^{*}\left(1 + \frac{2\xi_j}{h_c}\right)FG - V \tag{42e}$$

$$V_{CNT} = V_{CNT}^{*}\left(1 - \frac{2\xi_j}{h_c}\right)FG - A \tag{42f}$$

$$V_{CNT} = V_{CNT}^{*}FG - U \tag{42g}$$

Also, For $j = 1,2,\ldots,N_t, \xi_j = \left(\frac{1}{2} + \frac{1}{2N_t} - \frac{j}{N_t}\right)h_c$. The total volume fraction can be defined as follows:

$$V_{CNT} + V_M = 1 \tag{43}$$

The effective density as well as Poisson ratio of the nanocomposite matrix can be written as

$$\rho^{NCM} = V_M\rho^M + V_{CNT}\rho^{CNT} \tag{44a}$$

$$\nu^{NCM} = \nu^M \tag{44b}$$

4. Solution procedure

In this research, the governing equation and boundary conditions are solved using the generalized differential quadrature method (GDQM) (Liu *et al*. 2020a, Wang *et al*. 2020, Zhou *et al*. 2020, Dai *et al*. 2021a, Guo *et al*. 2021a, Shao *et al*. 2021, Wu and Habibi 2021), which is a numerical solution method for higher-order equations. The r-th order derivative of $\Psi(x_i)$, is expressed as follows using the sixth order GDQM technique (Wu and Liu 2000).

$$\begin{aligned}\Psi^{(r)}(x_i) &= \sum_{k=0}^{2} h_{1k}^{(r)}(x_i)\Psi_1^{(k)} + \sum_{j=2}^{ns-1} h_{j0}^{(r)}(x_i)\Psi_j \\ &+ \sum_{k=0}^{2} h_{nsk}^{(r)}(x_i)\Psi_{ns}^{(k)} = \sum_{j=1}^{ns+4}\beta_{ij}^{(r)}U_j^w \ (i = 1,2,\ldots,ns)\end{aligned} \tag{45}$$

where x_i, $\beta_{ijl}^{(r)}$, ns, and $h_{jl}^{(r)}(x_i)$ denote the sampling point positions, the r-th order derivative at each x_i, sampling point number, and shape functions of hermit interpolation. Also, the discrete type of deformation, V_j, should be considered as

$$\begin{aligned}&\{U^w\}^T \\ &= \left\{\Psi_1^{(0)}, \Psi_1^{(1)}, \Psi_1^{(2)}, \Psi_2, \Psi_3, \ldots, \Psi_{ns-1}, \Psi_{ns}^{(0)}, \Psi_{ns}^{(1)}, \Psi_{ns}^{(2)}\right\} \\ &= \{U_1^w, U_2^w, \ldots, U_{ns+4}^w\}\end{aligned} \tag{46}$$

Sampling points, according to Chebyshev Gauss Lobatto, can be assumed as

$$x_i = \frac{L}{2}\left[1 - cos\left(\frac{(i-1)}{(ns-1)}\pi\right)\right](i = 1,2,\ldots,ns) \tag{47}$$

in addition, shape functions related to Hermite interpolation are

$$\beta_{ijl}^{(r)} = h_{jl}^{(r)}(x_i) = \frac{d^r h_{jl}(x_i)}{dx^r} \tag{48}$$

In which

$$h_{jl}^{(r)}(x_i) = \begin{cases}1 \text{ if } i = j \quad l = r \\ 0 \text{ otherwise}\end{cases} \tag{49a}$$

$$h_{pi}(x) = \frac{(x - x_{(ns+1)-p})}{(x_1 - x_{ns})}(a_{pi}x^2 + b_{pi}x + c_{pi})l_p(x) \tag{49b}$$
(p=1, ns and $i = 0,1,2$)

$$h_{j0}(x) = \frac{(x - x_1)^2(x - x_{ns})^2}{(x_j - x_1)^2(x_j - x_{ns})^2}l_j(x) \tag{49c}$$
$(j = 2,3,\ldots,ns-1)$

where a_{pi}, b_{pi} and c_{pi} are the constant coefficients which are expressed in appendix-I. Additionally, the test functions associated with Lagrangian interpolation, $l_j(x_i)$, are equal to Dirac delta (δ_{ij}). Also, the first derivative of weighting coefficient can be expressed as the following equation (Hamidian *et al*. 2011, Shariati 2008, Shariati *et al*. 2011, 2018, 2019, 2020d, Shah *et al*. 2015, 2016a, b, Khanouki *et al*. 2016, Toghroli *et al*. 2017, 2018, 2020, Chen *et al*. 2019, Li *et al*. 2019, Naghipour *et al*. 2020, Razavian *et al*. 2020, Hosseini and Toghroli 2021, Mehrabi *et al*. 2021).

$$l_j^{(1)}(x_i) = \begin{cases}\dfrac{R^{(1)}(x_i)}{(x_i - x_j)R^{(1)}(x_j)} \text{ (for } i,j = 1,2,\ldots,ns, i \neq j) \\ -\displaystyle\sum_{j=1,i\neq j}^{ns} l_j^{(1)}(x_i) \text{ (for } i,j = 1,2,\ldots,ns)\end{cases} \tag{50}$$

where

$$R^{(1)}(x_i) = \prod_{m=1,m\neq i}^{ns}(x_i - x_m) \tag{51}$$

Additionally, higher order derivatives related to the Lagrangian interpolation test functions are defined as (Wang *et al*. 2021, Shi *et al*. 2022, Xie and Chen 2022).

$$l_j^{(r)}(x_i) = \begin{cases}r\left(l_i^{(r-1)}(x_i)l_j^{(1)}(x_i) - \dfrac{l_j^{(r-1)}(x_i)}{(x_i - x_j)}\right) \\ \text{(for } i,j = 1,2,\ldots,ns) \\ -\displaystyle\sum_{j=1,i\neq j}^{ns} l_j^{(r)}(x_i) \text{ (for } i,j = 1,2,\ldots,ns)\end{cases} \tag{52}$$

Also, separation of variables for electric potential as well as is expressed as follows.

$$\phi^t(x,t) = \Phi^t(x)e^{i\lambda t} \tag{53a}$$

$$\phi^b(x,t) = \Phi^b(x)e^{i\lambda t} \tag{53b}$$

$$R(x,t) = \bar{R}(x)e^{i\lambda t} \tag{53c}$$

Because the electric potential equation order is two, DQM is used as follow

$$U^{(r)}(x_i) = \sum_{j=1}^{ns} l_{ij}^{(r)} U_j \ (i = 1,2,\dots,ns) \tag{54}$$

The discrete form of displacement, elastic foundation force, as well as electric potential are defined as follows:

$$\{U^w\}^T = \{U_1^w, U_2^w, \dots, U_{ns+4}^w\}^T \tag{55a}$$

$$\{U^t\}^T = \left\{\phi^t{}_1, \dots, \phi^t{}_{ns}\right\}^T \tag{55a}$$

$$\{U^b\}^T = \left\{\phi^b{}_1, \dots, \phi^b{}_{ns}\right\}^T \tag{55c}$$

$$\left\{U^{\bar{R}}\right\}^T = \left\{\bar{R}_{\ 1}, \dots, \bar{R}_{\ ns}\right\}^T \tag{55d}$$

Now, using Eqs. (22), (27), (28), (45), (54), and (55), all formulation can be summarized as below

$$\begin{bmatrix} M_{ww} & 0 & 0 & 0 \\ 0 & 0 & 0 & 0 \\ 0 & 0 & 0 & 0 \\ 0 & 0 & 0 & 0 \end{bmatrix} \{\ddot{X}\} + \begin{bmatrix} K_{ww} & K_{w\phi^t} & K_{w\phi^b} & K_{wR} \\ K_{\phi^t w} & K_{\phi^t\phi^t} & 0 & 0 \\ K_{\phi^b w} & 0 & K_{\phi^b\phi^b} & 0 \\ K_{Rw} & 0 & 0 & K_{RR} \end{bmatrix} \{X\} = \{F\} \tag{56}$$

where

$$\{X\} = \{U^w \quad U^t \quad U^b \quad U^R\} \tag{57}$$

According to the third row of Eq. (56)

$$U^b = -{K_{\phi^b\phi^b}}^{-1} K_{\phi^b w} U^w \tag{58}$$

And using a PD controller as

$$U^t = G_c U^b + G_v \dot{U}^b \tag{59}$$

Therefore, the equivalent stiffness, damping, and mass matrix for a controlled system can be defined as follow

$$[M] = M_{ww} \tag{60a}$$

$$[K] = K_{ww} + K_{w\phi^b}\left(-{K_{\phi^b\phi^b}}^{-1} K_{\phi^b w}\right) + G_c K_{w\phi^t}\left(-{K_{\phi^b\phi^b}}^{-1} K_{\phi^b w}\right) + K_{wR}\left(-{K_{RR}}^{-1} K_{Rw}\right) \tag{60b}$$

$$[C] = C_{ww} + G_v K_{w\phi^t}\left(-{K_{\phi^b\phi^b}}^{-1} K_{\phi^b w}\right) \tag{60c}$$

where

$$C_{ww} = \beta[K] + \alpha[M] \tag{61}$$

where

$$\alpha = 2\xi_i \left(\frac{\omega_i \omega_j}{\omega_i + \omega_j}\right) \tag{62a}$$

$$\beta = 2\xi_i \left(\frac{1}{\omega_i + \omega_j}\right) \tag{62b}$$

In which ξ_i is damping ratio and ω_i is the natural frequency. Also, for an uncontrolled system, the stiffness, damping, and mass matrix may be represented as follows:

$$[M] = M_{ww} \tag{63a}$$

$$[K] = K_{ww} + K_{w\phi^b}\left(-{K_{\phi^b\phi^b}}^{-1} K_{\phi^b w}\right) + K_{w\phi^t}\left(-{K_{\phi^t\phi^t}}^{-1} K_{\phi^t w}\right) + K_{wR}\left(-{K_{RR}}^{-1} K_{Rw}\right) \tag{63b}$$

$$[C] = C_{ww} \tag{63c}$$

The forced vibration findings are obtained using the Newmark beta technique. Based on this method, the differential equation as below can be solved.

$$[M]\{\ddot{U}^w\} + [C]\{\dot{U}^w\} + [K]\{U^w\} = \{F\} \tag{64}$$

where denote $[K], [C]$, and $[M]$ stiffness matrix, damping matrix, and mass matrix obtained in previous sections. By introducing the effective stiffness matrix $[\bar{K}]$ and effective force vector $\{\bar{F}_{t+\Delta t}\}$ as the following matrix, the displacement vector at each time $\{U^w{}_{t+\Delta t}\}$can be obtained.

$$[\bar{K}] = [K] + a_0[M] + a_1[C] \tag{65a}$$

$$\{\bar{F}_{t+\Delta t}\} = \{F_{t+\Delta t}\} + [M]\left(a_0\{U_t^w\} + a_2\{\dot{U}^w{}_t\} + a_3\{\ddot{U}^w{}_t\}\right) + [C]\left(a_1\{U_t^w\} + a_4\{\dot{U}^w{}_t\} + a_5\{\ddot{U}^w{}_t\}\right) \tag{65b}$$

$$\{U^w{}_{t+\Delta t}\} = [\bar{K}]^{-1}\{\bar{F}_{t+\Delta t}\} \tag{65c}$$

Also, the velocity vector can be attained as

$$\{\dot{U}^w{}_{t+\Delta t}\} = a_1(\{U^w{}_{t+\Delta t}\} - \{U^w{}_t\}) - a_4\{\dot{U}^w{}_t\} - a_5\{\ddot{U}^w{}_t\} \tag{66}$$

and also, the acceleration vector at each time can be expressed as follow

$$\{\ddot{U}^w{}_{t+\Delta t}\} = a_0(\{U^w{}_{t+\Delta t}\} - \{U^w{}_t\}) - a_2\{\dot{U}^w{}_t\} - a_3\{\ddot{U}^w{}_t\} \tag{67}$$

where the time intervals and constants are defined as regards:

$$a_0 = \frac{1}{\beta(\Delta t)^2} \tag{68a}$$

$$a_1 = \frac{\alpha}{\beta \Delta t} \tag{68b}$$

$$a_2 = \frac{1}{\beta \Delta t} \tag{68c}$$

$$a_3 = \frac{1}{2\beta} - 1 \tag{68d}$$

$$a_4 = \frac{\alpha}{\beta} - 1 \tag{68e}$$

$$a_4 = \frac{\Delta t}{2}\left(\frac{\alpha}{\beta} - 2\right) \tag{68f}$$

where, α=1/2 and β=1/4.

Table 1 The first two non-dimensional vibration frequencies of system including three layers with neglecting the piezoelectric effect for various values of ζ and $\frac{k}{L} = 0.05$

		Modes					
		1st			2nd		
B.Cs	ζ	Fernández-Sáez and Zaera (2017)	Exact Fernández-Sáez and Zaera (2017)	Present-GDQM	Fernández-Sáez and Zaera (2017)	Exact Fernández-Sáez and Zaera (2017)	Present-GDQM
CF	1.00	3.5160	3.5160	3.4701	22.0344	22.0345	22.0269
	0.50	3.4105	3.4173	3.3945	21.2628	21.2626	21.2589
	0.10	3.2874	3.2908	3.2867	20.2713	20.3538	20.3531
	0.05	-	3.2617	3.2611	-	20.1592	20.1572
SS	1.00	9.8696	9.8696	9.8696	39.4784	39.4784	39.4784
	0.50	9.8192	9.8148	9.8149	38.6493	38.6502	38.6501
	0.10	9.7610	9.7671	9.7672	37.8993	37.9218	37.9218
	0.05	-	9.7601	9.7601	-	37.8150	37.8150
	0.01	-	9.7533	9.7534	-	37.7125	37.7126

*Notice that the values related to Ref. Fernández-Sáez and Zaera (2017) are obtained approximately from its figures.
**The exact values are attained by using the procedure which is presented by Fernández-Sáez and Zaera (2017).

Table 2 The first and second non-dimensional natural frequency of two-phase nanobeam including two piezoelectric layers and a nonpiezoelectric layer beam with $h_c = 0$ and for different boundary conditions, ζ, and $\frac{\kappa}{L}$

		1st mode				2nd mode			
		$\frac{\kappa}{L}$							
B.Cs	ζ	0.05		0.075		0.05		0.075	
		Present	Naderi *et al*. (2021)	Present	Naderi *et al*. (2021)	Present	Naderi *et al*. (2021)	Present	Naderi *et al*. (2021)
C-F	0.50	3.4246	3.4473	3.3486	3.4011	21.4450	21.4490	21.0042	21.0131
	0.10	3.3156	3.3197	3.2068	3.2170	20.5313	20.5323	19.6286	19.6305
	0.05	20.3336	3.2903	3.1703	3.1751	3.2897	20.3360	19.3447	19.3459
	0.01		3.2516		3.1203		20.0865		18.9922
C-C	0.50	21.2000	21.1999	20.544	20.5443	57.6208	57.6209	55.2802	55.2802
	0.10	19.5940	19.5936	18.265	18.2650	52.6100	52.6100	47.9872	47.9872
	0.05	19.2490	19.2485	17.795	17.7948	51.6100	51.6100	46.6133	46.6133
	0.01	18.808	18.8082	17.206	17.2064	50.3825	50.3830	44.9871	44.9871
C-S	0.50	15.0220	15.0223	14.7290	14.7288	47.9672	47.9672	46.4480	46.4487
	0.10	14.3910	14.3906	13.7810	13.7808	45.3566	45.3566	42.3247	42.3247
	0.05	14.253	14.2535	13.5820	13.5817	44.8469	44.8469	41.5568	41.5568
	0.01	14.0780	14.0779	13.3310	13.3307	44.2301	44.2310	40.6592	40.6592
S-S	0.50	9.9009	9.9009	9.8401	9.8403	38.9891	38.9891	38.1665	38.1664
	0.10	9.8528	9.8528	9.7342	9.7342	38.2544	38.2544	36.6337	36.6337
	0.05	9.8457	9.8457	9.7175	9.7175	38.1466	38.1466	36.3945	36.3945
	0.01	9.8389	9.8389	9.7004	9.7004	38.0433	38.0433	36.1534	36.1534

5. Numerical results

In the following, the numerically calculated results are validated and discussed in detail in order to investigate the various impacts on the energy harvesting of the dynamic behavior of piezoelectric bi-layered composite nanoscale beam on the basis of the classical beam theory in two phases of the elastic medium under the shockwave force using a couple of generalized differential quadrature method and Newmark-beta approach. Accordingly, the system containing one core layer made of Aluminum $\rho = 2700\left(\frac{Kg}{m^3}\right)$, $E = 69(GPa)$, $h_c = 0.05L$, and two piezoelectric layers with $\rho = 7500\left(\frac{Kg}{m^3}\right)$, $E = 132(GPa)$, $L = 200(nm)$, $h_b = h_t = 0.0125L$, $e = -4.1\left(\frac{C}{m^2}\right)$, and $\eta = 7.124\left(\frac{N}{m^2K}\right)$. Also, the damping ratio is $\xi_i = 0.05$, and the explosion details

Table 3 The first two nondimensional frequency for a beam constitutes of three layers whose piezoelectricity is neglected and is rested on an elastic foundation for various ζ and $\frac{\kappa}{L}$

BCs.	ζ	$\frac{\kappa}{L}$ 0.05		0.075		0.1	
		Present	Fakher *et al.* (2020)	Present	Fakher *et al.* (2020)	Present	Fakher *et al.* (2020)
SS	0.5	13.9730	13.9730	13.8890	13.8885	13.7850	13.7846
	0.1	13.9080	13.9083	13.7490	13.7493	13.5490	13.5494
	0.01	13.8920	13.8916	13.7110	13.7112	13.4810	13.4811
CF	0.5	10.3280	10.3359	10.1920	10.2098	10.0570	10.0891
	0.1	10.1070	10.1084	9.8707	9.8742	9.6425	9.6489
	0.01	10.2540	10.0472	9.7986	9.7863	9.5372	9.5362

are $\tilde{R} = 0.1(m)$,$\widetilde{W} = 1(Kg)$, and $P_0 = 10^4(Pa)$. In addition, the values related to nanocomposite materials are $E^M = 3.51(GPa)$, $\rho^M = 1200\left(\frac{Kg}{m^3}\right)$, $\nu^M = 0.34$, $E_{11}^F = 233.05\ (GPa)$, $\nu^F = 0.2, \rho^F = 1750\left(\frac{Kg}{m^3}\right), E_{11}^{CNT} = 640(GPa)$, $\nu^{CNT} = 0.175$, $\rho^{CNT} = 1350\left(\frac{Kg}{m^3}\right)$, $d^{CNT} = 1.4 \times 10^{-3}(nM)$, $l^{CNT} = 0.25(nM)$, and $t^{CNT} = 0.34 \times 10^{-3}(nM)$.

5.1 Comparison study

Before looking into the results, it is essential to compare them to earlier researchs. The first and second nondimensional vibration frequencies of clamped-free (CF) and fully simply supported (SS) beams are compared in Table 1, in order to the findings obtained by Fernández-Sáez and Zaera (2017) to verify the formulation and solution methodology for a system that contains a core beam layer and two piezoelectric layers at the top and bottom of the core. A comparison of the reported results confirms that the proposed governing equations and solution technique are well validated.

Then, to validate the results for modeling the piezoelectric layers, with setting the thickness of the core layer to zero ($h_c = 0$), the first two non-dimensional ($\Gamma = \omega L^2\sqrt{\frac{m_1}{D_{11}}}$) vibration frequency for various boundary conditions involving clamped-free (C-F), fully clamped (C-C), fully simply supported (S-S), and clamped-simply supported, are attained and compared with the results of Naderi *et al.* (2021) in Table 2, which an excellent agreement between the results can be detected.

Ultimately, to examine the validity of the elastic foundation, by eliminating the piezoelectricity, the first two dimensionless frequencies ($\Gamma = \omega L^2\sqrt{\frac{m_1}{D_{11}}}$) of a beam rested on an elastic foundation for two types of boundary conditions (S-S and C-F), various values of ,ξ, and ,κ/L,, and constant value of ,k*f*=100,, is obtained and compared with results of Fakher *et al.* (2020) in Table 3, and the excellent validation is done by examining the manifested results. Based on the comparisons in Table 1, Table 2, and Table 3, it is obvious that the formulation and solution approach are acceptable for investigating a three-layer

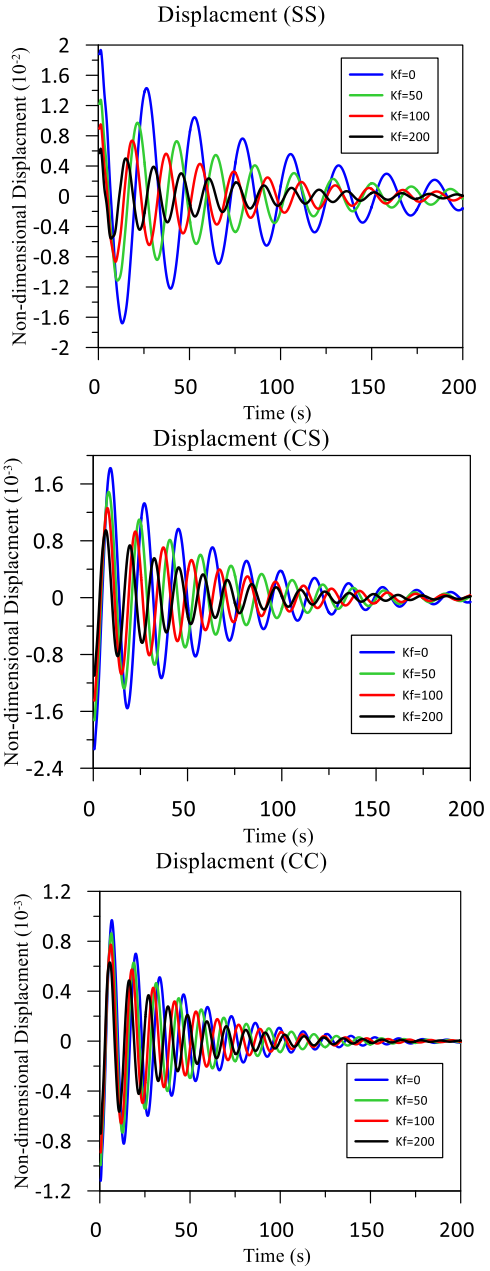

Fig. 3 The nondimensional displacement of the middle of a nanobeam subjected to a shockwave and rested on elastic foundation versus time

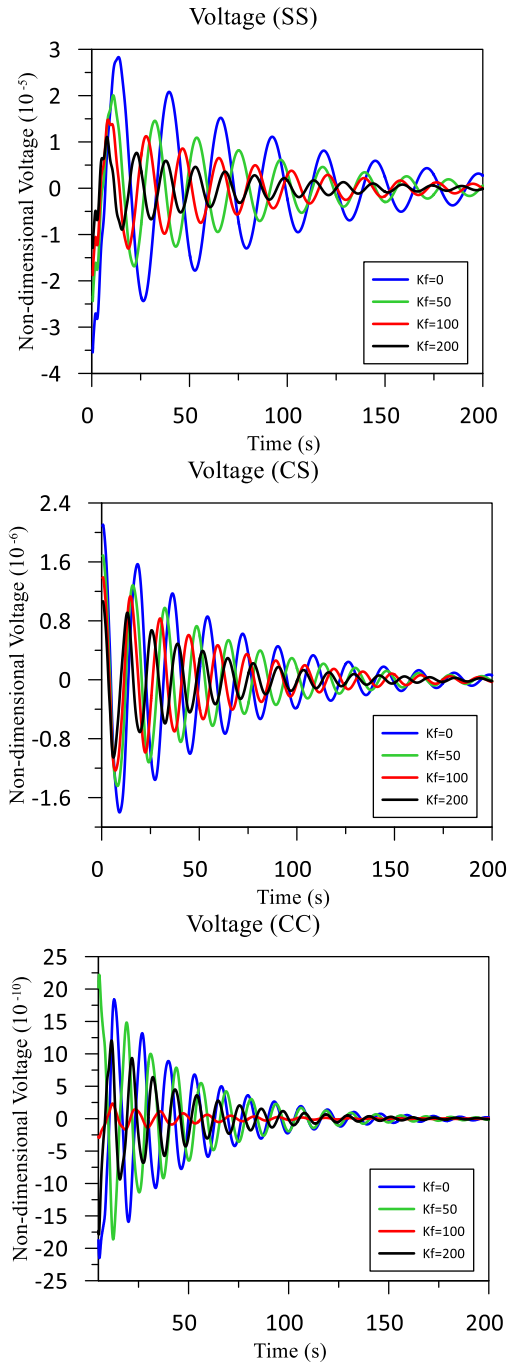

Fig. 4 The nondimensional voltage of a nanobeam containing a core layer as well as two piezoelectric layers subjected to a shockwave versus time

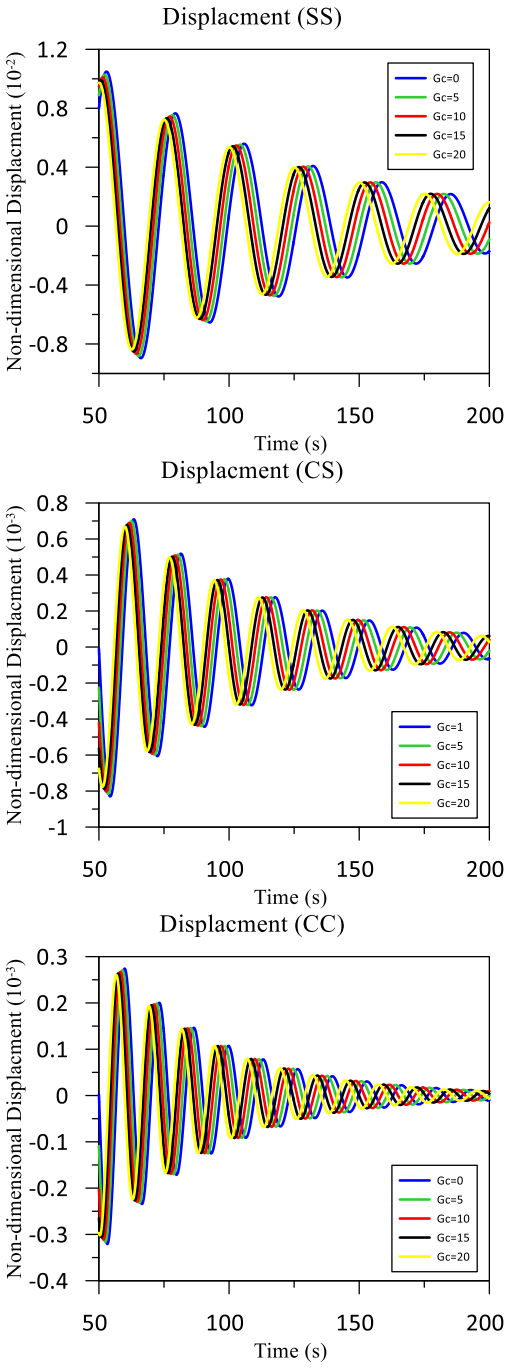

Fig. 5 The controlled time response of a three layers beam with different boundry conditions as well as various controller gain values G_c

system with one core and two piezoelectric layers resting on an elastic foundation.

5.2 Results and discussion

The findings of forced vibration, dynamic stability, and energy harvesting are now achieved using the Newmark beta technique. To begin, the impact of foundation on energy harvesting and deflection of a nanobeam with constant values of $\zeta = 0.1$ and $\frac{\kappa}{L} = 0.05$ is evaluated by plotting the nondimensional deflection of the beams mid-point exposed to a shock wave against time for various values of K_f and varied boundary conditions in Fig. 3. As shown in Fig. 3, the stiffer the foundation, the less the displacement of the nanobeam. It should also be noted that the effect of foundation is greater when the border condition is softer, i.e., SS. Furthermore, overall deflection is smaller under stiffer boundary circumstances than in softer boundary conditions.

Next, the effect of foundation on nondimensional voltage response of the system including a core layer and two piezoelectric layers subjected to a blast load is

investigated. To do so, the voltage harvested from a nanobeam with constant values of $\zeta = 0.1$ and $\frac{\kappa}{L} = 0.05$ which is subjected to a shockwave for different values of K_f and various boundary conditions is plotted in Fig. 4. According to Fig. 4, the stronger foundation causes the beam to have less deflection, which lowers the voltage that can be collected from the system. It is also worth noting that the potential of collecting more voltage increases under softer boundary conditions.

The temporal response of the midpoint of the beam exposed to a blast load for various boundary conditions with varied controller values G_c and constant $G_v = 0$, $K_f = 0, \zeta = 0.1$ and $\frac{\kappa}{L} = 0.05$ value of is shown in Fig. 5 in order to examine the impact of controller on the vibration displacement of the beam. It can be seen from Fig. 5 that, G_c, can cause the beam to have less amplitude, and also, it shifts the responsibility to dampen the initial deflection faster. Also, it can be observed that the effect is more when the boundary condition is stiffer.

6. Conclusions

Using paradox-free local/nonlocal theory, the feasibility of energy harvesting as well as controlled vibration of a three-layered beam consisting of two piezoelectric layers and one core layer comprised of nonpiezoelectric material was examined. A blast load has been applied to the three-layered nanobeam, which is sitting on an elastic basis. In addition, the core layer was constructed of Nanocomposites that were reinforced with carbon nanotubes and carbon fibers (MHCD). Hamilton,s concept has been used to find governing equations and boundary conditions. The equations were discretized using the Generalized Differential Quadrature Technique (GDQM), and the Newmark beta method was used to solve them. In addition, the forced vibration was controlled by two differential and integral gains. Two-phase elasticity has been used to model the elastic foundation,s size dependence. The influence of elastic foundations, control gains, nonlocal factors, and core material properties on forced vibration and energy harvesting was examined. Some compassion studies have been used to verify the equations and solution technique.

References

Adamian, A., Safari, K.H., Sheikholeslami, M., Habibi, M., Al-Furjan, M. and Chen, G. (2020), "Critical temperature and frequency characteristics of GPLs-reinforced composite doubly curved panel", *Appl. Sci.*, **10**(9), 3251. https://doi.org/10.3390/app10093251

Adhikari, S., Gilchrist, D., Murmu, T. and McCarthy, M. (2015), "Nonlocal normal modes in nanoscale dynamical systems", *Mech. Syst. Signal Pr.*, **60**, 583-603. https://doi.org/10.1016/j.ymssp.2014.12.004

Akbaş, Ş.D. (2018a), "Bending of a cracked functionally graded nanobeam", *Adv. Nano Res.*, **6**(3), 219. http://doi.org/10.12989/anr.2018.6.3.219

Akbaş, Ş.D. (2018b), "Forced vibration analysis of cracked functionally graded microbeams", *Adv. Nano Res.*, **6**(1), 39. http://doi.org/10.12989/anr.2018.6.1.039

Al-Furjan, M., Dehini, R., Khorami, M., Habibi, M. and won Jung, D. (2020a), "On the dynamics of the ultra-fast rotating cantilever orthotropic piezoelectric nanodisk based on nonlocal strain gradient theory", *Compos. Struct.*, 112990. https://doi.org/10.1016/j.compstruct.2020.112990

Al-Furjan, M., Fereidouni, M., Habibi, M., Abd Ali, R., Ni, J. and Safarpour, M. (2020b), "Influence of in-plane loading on the vibrations of the fully symmetric mechanical systems via dynamic simulation and generalized differential quadrature framework", *Eng. Comput.*, 1-23. https://doi.org/10.1007/s00366-020-01177-7

Al-Furjan, M., Fereidouni, M., Sedghiyan, D., Habibi, M. and won Jung, D. (2020c), "Three-dimensional frequency response of the CNT-Carbon-Fiber reinforced laminated circular/annular plates under initially stresses", *Compos. Struct.*, 113146. https://doi.org/10.1016/j.compstruct.2020.113146

Al-Furjan, M., Habibi, M., won Jung, D. and Safarpour, H. (2020d), "Vibrational characteristics of a higher-order laminated composite viscoelastic annular microplate via modified couple stress theory", *Compos. Struct.*, 113152. https://doi.org/10.1016/j.compstruct.2020.113152

Al-Furjan, M., Moghadam, S.A., Dehini, R., Shan, L., Habibi, M. and Safarpour, H. (2020e), "Vibration control of a smart shell reinforced by graphene nanoplatelets under external load: Semi-numerical and finite element modeling", *Thin Wall. Struct.*, 107242. https://doi.org/10.1016/j.tws.2020.107242

Al-Furjan, M., Oyarhossein, M.A., Habibi, M., Safarpour, H. and Jung, D.W. (2020f), "Frequency and critical angular velocity characteristics of rotary laminated cantilever microdisk via two-dimensional analysis", *Thin Wall. Struct.*, **157**, 107111. https://doi.org/10.1016/j.tws.2020.107111

Alipour, M., Torabi, M.A., Sareban, M., Lashini, H., Sadeghi, E., Fazaeli, A., Habibi, M. and Hashemi, R. (2020), "Finite element and experimental method for analyzing the effects of martensite morphologies on the formability of DP steels", *Mech. Based Des. Struct.*, **48**(5), 525-541. https://doi.org/10.1080/15397734.2019.1633343

Allahkarami, F., Nikkhah-Bahrami, M. and Saryazdi, M.G. (2017), "Damping and vibration analysis of viscoelastic curved microbeam reinforced with FG-CNTs resting on viscoelastic medium using strain gradient theory and DQM", *Steel. Compos. Struct.*, **25**(2), 141-155. https://doi.org/10.12989/scs.2017.25.2.141

Apuzzo, A., Barretta, R., Luciano, R., de Sciarra, F.M. and Penna, R. (2017), "Free vibrations of Bernoulli-Euler nano-beams by the stress-driven nonlocal integral model", *Compos. Part B Eng.*, **123**, 105-111. https://doi.org/10.1016/j.compositesb.2017.03.057

Arefi, M. and Zenkour, A.M. (2018), "Free vibration analysis of a three-layered microbeam based on strain gradient theory and three-unknown shear and normal deformation theory", *Steel. Compos. Struct.*, **26**(4), 421-437. https://doi.org/10.12989/scs.2018.26.4.421

Aydogdu, M., Arda, M. and Filiz, S. (2018), "Vibration of axially functionally graded nano rods and beams with a variable nonlocal parameter", *Adv. Nano Res.*, **6**(3), 257. http://doi.org/10.12989/anr.2018.6.3.257

Bai, B., Jiang, S., Liu, L., Li, X. and Wu, H. (2021), "The transport of silica powders and lead ions under unsteady flow and variable injection concentrations", *Powder Technol.*, **387**, 22-30. https://doi.org/10.1016/j.powtec.2021.04.014

Bai, Y., Alzahrani, B., Baharom, S. and Habibi, M. (2020), "Semi-numerical simulation for vibrational responses of the viscoelastic imperfect annular system with honeycomb core under residual pressure", *Eng. Comput.*, 1-26. https://doi.org/10.1007/s00366-020-01191-9

Behdad, S., Fakher, M. and Hosseini-Hashemi, S. (2021), "Dynamic stability and vibration of two-phase local/nonlocal VFGP nanobeams incorporating surface effects and different boundary conditions", *Mech. Mater.*, **153**, 103633. https://doi.org/10.1016/j.mechmat.2020.103633

Bensaid, I., Bekhadda, A. and Kerboua, B. (2018), "Dynamic analysis of higher order shear-deformable nanobeams resting on elastic foundation based on nonlocal strain gradient theory", *Adv. Nano Res.*, **6**(3), 279. http://doi.org/10.12989/anr.2018.6.3.279

Challamel, N. and Wang, C. (2008), "The small length scale effect for a non-local cantilever beam: A paradox solved", *Nanotechnology*, **19**(34), 345703. https://doi.org/10.1088/0957-4484/19/34/345703

Challamel, N., Zhang, Z., Wang, C., Reddy, J., Wang, Q., Michelitsch, T. and Collet, B. (2014), "On nonconservativeness of Eringen,s nonlocal elasticity in beam mechanics: correction from a discrete-based approach", *Arch. Appl. Mech.*, **84**(9), 1275-1292. https://doi.org/10.1007/s00419-014-0862-x

Chen, C., Shi, L., Shariati, M., Toghroli, A., Mohamad, E.T., Bui, D.T. and Khorami, M. (2019), "Behavior of steel storage pallet racking connection-A review", *Steel. Compos. Struct.*, **30**(5), 457. https://doi.org/10.12989/scs.2019.30.5.457

Chen, F., Chen, J., Duan, R., Habibi, M. and Khadimallah, M.A. (2022), "Investigation on dynamic stability and aeroelastic characteristics of composite curved pipes with any yawed angle", *Compos. Struct.*, 115195. https://doi.org/10.1016/j.compstruct.2022.115195

Cheshmeh, E., Karbon, M., Eyvazian, A., Jung, D.w., Habibi, M. and Safarpour, M. (2020), "Buckling and vibration analysis of FG-CNTRC plate subjected to thermo-mechanical load based on higher order shear deformation theory", *Mech. Based Des. Struct.*, 1-24. https://doi.org/10.1080/15397734.2020.1744005

Dai, Z., Jiang, Z., Zhang, L. and Habibi, M. (2021a), "Frequency characteristics and sensitivity analysis of a size-dependent laminated nanoshell", *Adv. Nano Res.*, **10**(2), 175. https://doi.org/10.12989/anr.2021.10.2.175

Dai, Z., Zhang, L., Bolandi, S.Y. and Habibi, M. (2021b), "On the vibrations of the non-polynomial viscoelastic composite open-type shell under residual stresses", *Compos. Struct.*, 113599. https://doi.org/10.1016/j.compstruct.2021.113599

Dong, Y., Gao, Y., Zhu, Q., Moradi, Z. and Safa, M. (2022), "TE-GDQE implementation to investigate the vibration of FG composite conical shells considering a frequency controller solid ring", *Eng. Anal. Bound. Elem.*, **138**, 95-107. https://doi.org/10.1016/j.enganabound.2022.01.017

Ebrahimi, F. and Barati, M.R. (2017), "Buckling analysis of nonlocal third-order shear deformable functionally graded piezoelectric nanobeams embedded in elastic medium", *J. Brazil. Soc. Mech. Sci. Eng.*, **39**(3), 937-952. https://doi.org/10.1007/s40430-016-0551-5

Ebrahimi, F., Barati, M.R. and Haghi, P. (2018), "Wave propagation analysis of size-dependent rotating inhomogeneous nanobeams based on nonlocal elasticity theory", *J. Vib. Control*, **24**(17), 3809-3818. https://doi.org/10.1177/1077546317711537

Ebrahimi, F., Habibi, M. and Safarpour, H. (2019a), "On modeling of wave propagation in a thermally affected GNP-reinforced imperfect nanocomposite shell", *Eng. Comput.*, **35**(4), 1375-1389. https://doi.org/10.1007/s00366-018-0669-4

Ebrahimi, F., Hajilak, Z.E., Habibi, M. and Safarpour, H. (2019b), "Buckling and vibration characteristics of a carbon nanotube-reinforced spinning cantilever cylindrical 3D shell conveying viscous fluid flow and carrying spring-mass systems under various temperature distributions", *Proceedings of the Institution of Mechanical Engineers, Part C: Journal of Mechanical Engineering Science*, **233**(13), 4590-4605. https://doi.org/10.1177/0954406219832323

Ebrahimi, F., Hashemabadi, D., Habibi, M. and Safarpour, H. (2020a), "Thermal buckling and forced vibration characteristics of a porous GNP reinforced nanocomposite cylindrical shell", *Microsyst. Technol.*, **26**(2), 461-473. https://doi.org/10.1007/s00542-019-04542-9

Ebrahimi, F., Kokaba, M., Shaghaghi, G. and Selvamani, R. (2020b), "Dynamic characteristics of hygro-magneto-thermo-electrical nanobeam with non-ideal boundary conditions", *Adv. Nano Res.*, **8**(2), 169-182. https://doi.org/10.12989/anr.2020.8.2.169

Ebrahimi, F., Mohammadi, K., Barouti, M.M. and Habibi, M. (2019c), "Wave propagation analysis of a spinning porous graphene nanoplatelet-reinforced nanoshell", *Waves Random Complex Med.*, 1-27. https://doi.org/10.1080/17455030.2019.1694729

Ebrahimi, F., Supeni, E.E.B., Habibi, M. and Safarpour, H. (2020c), "Frequency characteristics of a GPL-reinforced composite microdisk coupled with a piezoelectric layer", *Eur. Phys. J. Plus*, **135**(2), 144. https://doi.org/10.1140/epjp/s13360-020-00217-x

Ehyaei, J., Akbarshahi, A. and Shafiei, N. (2017), "Influence of porosity and axial preload on vibration behavior of rotating FG nanobeam", *Adv. Nano Res.*, **5**(2), 141. http://doi.org/10.12989/anr.2017.5.2.141

Eringen, A.C. (1972), "Nonlocal polar elastic continua", *Int. J. Eng. Sci.*, **10**(1), 1-16. https://doi.org/10.1016/0020-7225(72)90070-5

Eringen, A.C. (1983), "On differential equations of nonlocal elasticity and solutions of screw dislocation and surface waves", *J. Appl. Phys.*, **54**(9), 4703-4710. https://doi.org/10.1063/1.332803

Eringen, A.C. and Edelen, D. (1972), "On nonlocal elasticity", *Int. J. Eng. Sci.*, **10**(3), 233-248. https://doi.org/10.1016/0020-7225(72)90039-0

Esmailpoor Hajilak, Z., Pourghader, J., Hashemabadi, D., Sharifi Bagh, F., Habibi, M. and Safarpour, H. (2019), "Multilayer GPLRC composite cylindrical nanoshell using modified strain gradient theory", *Mech. Based Des. Struct.*, **47**(5), 521-545. https://doi/10.1080/15397734.2019.1566743

Fakher, M., Behdad, S., Naderi, A. and Hosseini-Hashemi, S. (2020), "Thermal vibration and buckling analysis of two-phase nanobeams embedded in size dependent elastic medium", *Int. J. Mech. Sci.*, **171**, 105381. https://doi.org/10.1016/j.ijmecsci.2019.105381

Fakher, M. and Hosseini-Hashemi, S. (2020a), "Nonlinear vibration analysis of two-phase local/nonlocal nanobeams with size-dependent nonlinearity by using Galerkin method", *J. Vib. Control*, 1077546320927619. https://doi.org/10.1177/1077546320927619

Fakher, M. and Hosseini-Hashemi, S. (2020b), "Vibration of two-phase local/nonlocal Timoshenko nanobeams with an efficient shear-locking-free finite-element model and exact solution", *Eng. Comput.*, 1-15. https://doi.org/10.1007/s00366-020-01058-z

Fan, L., Huang, Y., Ji, D., Moradi, Z., Safa, M. and Amine Khadimallah, M. (2022), "Interaction of angular velocity and temperature rise in the thermo-inertia bifurcation buckling of FG laminated nanocomposite annular plates", *Eng. Struct.*, **265**, 114518. https://doi.org/10.1016/j.engstruct.2022.114518

Fernández-Sáez, J. and Zaera, R. (2017), "Vibrations of Bernoulli-Euler beams using the two-phase nonlocal elasticity theory", *Int. J. Eng. Sci.*, **119**, 232-248. https://doi.org/10.1016/j.ijengsci.2017.06.021

Gafour, Y., Hamidi, A., Benahmed, A., Zidour, M. and Bensattalah, T. (2020), "Porosity-dependent free vibration analysis of FG nanobeam using non-local shear deformation and energy principle", *Adv. Nano Res.*, **8**(1), 37-47.

https://doi.org/10.12989/anr.2020.8.1.037

Gao, N., Zhang, Z., Deng, J., Guo, X., Cheng, B. and Hou, H. (2022), "Acoustic metamaterials for noise reduction: A review", *Adv. Mater. Technol.*, 2100698. https://doi.org/10.1002/admt.202100698

Ghazanfari, A., Soleimani, S.S., Keshavarzzadeh, M., Habibi, M., Assempuor, A. and Hashemi, R. (2020), "Prediction of FLD for sheet metal by considering through-thickness shear stresses", *Mech. Based Des. Struct.*, **48**(6), 755-772. https://doi.org/10.1080/15397734.2019.1662310

Guo, J., Baharvand, A., Tazeddinova, D., Habibi, M., Safarpour, H., Roco-Videla, A. and Selmi, A. (2021a), "An intelligent computer method for vibration responses of the spinning multi-layer symmetric nanosystem using multi-physics modeling", *Eng. Comput.*, 1-22. https://doi.org/10.1007/s00366-021-01433-4

Guo, Y., Mi, H. and Habibi, M. (2021b), "Electromechanical energy absorption, resonance frequency, and low-velocity impact analysis of the piezoelectric doubly curved system", *Mech. Syst. Signal Pr.*, **157**, 107723. https://doi.org/10.1016/j.ymssp.2021.107723

Habibi, M., Darabi, R., Sa, J.C.d. and Reis, A. (2021), "An innovation in finite element simulation via crystal plasticity assessment of grain morphology effect on sheet metal formability", *Proceedings of the Institution of Mechanical Engineers, Part L: Journal of Materials: Design and Applications*. **235**(8), 1937-1951. https://doi.org/10.1177/14644207211024686

Habibi, M., Ghazanfari, A., Assempour, A., Naghdabadi, R. and Hashemi, R. (2017), "Determination of forming limit diagram using two modified finite element models", *Mech. Eng.*, **48**(4), 141-144. https://doi.org/10.22060/MEJ.2016.664

Habibi, M., Hashemabadi, D. and Safarpour, H. (2019a), "Vibration analysis of a high-speed rotating GPLRC nanostructure coupled with a piezoelectric actuator", *Eur. Phys. J. Plus*, **134**(6), 307. https://doi.org/10.1140/epjp/i2019-12742-7

Habibi, M., Hashemi, R., Ghazanfari, A., Naghdabadi, R. and Assempour, A. (2018a), "Forming limit diagrams by including the M–K model in finite element simulation considering the effect of bending", *Proceedings of the Institution of Mechanical Engineers, Part L: Journal of Materials: Design and Applications*, **232**(8), 625-636.

Habibi, M., Hashemi, R., Sadeghi, E., Fazaeli, A., Ghazanfari, A. and Lashini, H. (2016), "Enhancing the mechanical properties and formability of low carbon steel with dual-phase microstructures", *J. Mater. Eng. Perform.*, **25**(2), 382-389.

Habibi, M., Hashemi, R., Tafti, M.F. and Assempour, A. (2018b), "Experimental investigation of mechanical properties, formability and forming limit diagrams for tailor-welded blanks produced by friction stir welding", *J. Manuf. Pr.*, **31**, 310-323.

Habibi, M., Mohammadgholiha, M. and Safarpour, H. (2019b), "Wave propagation characteristics of the electrically GNP-reinforced nanocomposite cylindrical shell", *J. Brazil. Soc. Mech. Sci. Eng.*, **41**(5), 221. https://doi.org/10.1007/s40430-019-1715-x

Habibi, M., Mohammadi, A., Safarpour, H. and Ghadiri, M. (2019c), "Effect of porosity on buckling and vibrational characteristics of the imperfect GPLRC composite nanoshell", *Mech. Based Des. Struct.*, 1-30.

Habibi, M., Mohammadi, A., Safarpour, H., Shavalipour, A. and Ghadiri, M. (2019d), "Wave propagation analysis of the laminated cylindrical nanoshell coupled with a piezoelectric actuator", *Mech. Based Des. Struct.*, 1-19. https://doi.org/10.1080/15397734.2019.1697932

Habibi, M., Safarpour, M. and Safarpour, H. (2020), "Vibrational characteristics of a FG-GPLRC viscoelastic thick annular plate using fourth-order Runge-Kutta and GDQ methods", *Mech. Based Des. Struct.*, 1-22. https://doi.org/10.1080/15397734.2020.1779086

Habibi, M., Taghdir, A. and Safarpour, H. (2019e), "Stability analysis of an electrically cylindrical nanoshell reinforced with graphene nanoplatelets", *Compos. Part. B Eng.*, **175**, 107125. https://doi.org/10.1016/j.compositesb.2019.107125

Hamidi, A., Houari, M.S.A., Mahmoud, S. and Tounsi, A. (2015), "A sinusoidal plate theory with 5-unknowns and stretching effect for thermomechanical bending of functionally graded sandwich plates", *Steel. Compos. Struct.*, **18**(1), 235-253. https://doi.org/10.12989/scs.2015.18.1.235

Hamidian, M., Shariati, M., Arabnejad, M. and Sinaei, H. (2011), "Assessment of high strength and light weight aggregate concrete properties using ultrasonic pulse velocity technique", *Int. J. Phys. Sci.*, **6**(22), 5261-5266. https://doi.org/10.5897/IJPS11.1081

Hashemi, H.R., Alizadeh, A.a., Oyarhossein, M.A., Shavalipour, A., Makkiabadi, M. and Habibi, M. (2019), "Influence of imperfection on amplitude and resonance frequency of a reinforcement compositionally graded nanostructure", *Waves Random Complex Med.*, 1-27. https://doi.org/10.1080/17455030.2019.1662968

He, X., Ding, J., Habibi, M., Safarpour, H. and Safarpour, M. (2021), "Non-polynomial framework for bending responses of the multi-scale hybrid laminated nanocomposite reinforced circular/annular plate", *Thin Wall. Struct.*, **166**, 108019. https://doi.org/10.1016/j.tws.2021.108019

Hosseini, S.A. and Toghroli, A. (2021), "Effect of mixing Nano-silica and Perlite with pervious concrete for nitrate removal from the contaminated water", *Adv. Concr. Constr.*, **11**(6), 531-544. https://doi.org/10.12989/acc.2021.11.6.531

Hou, F., Wu, S., Moradi, Z. and Shafiei, N. (2021), "The computational modeling for the static analysis of axially functionally graded micro-cylindrical imperfect beam applying the computer simulation", *Eng. Comput.*, 1-19.

Huang, X., Hao, H., Oslub, K., Habibi, M. and Tounsi, A. (2021a), "Dynamic stability/instability simulation of the rotary size-dependent functionally graded microsystem", *Eng. Comput.*, 1-17. https://doi.org/10.1007/s00366-021-01399-3

Huang, X., Zhang, Y., Moradi, Z. and Shafiei, N. (2021b), "Computer simulation via a couple of homotopy perturbation methods and the generalized differential quadrature method for nonlinear vibration of functionally graded non-uniform micro-tube", *Eng. Comput.*, 1-18. https://doi.org/10.1007/s00366-021-01395-7

Huang, X., Zhu, Y., Vafaei, P., Moradi, Z. and Davoudi, M. (2021c), "An iterative simulation algorithm for large oscillation of the applicable 2D-electrical system on a complex nonlinear substrate", *Eng. Comput.*, 1-13. https://doi.org/10.1007/s00366-021-01320-y

Jiang, L., Wang, Y., Wang, X., Ning, F., Wen, S., Zhou, Y., Chen, S., Betts, A., Jerrams, S. and Zhou, F.L. (2021), "Electro-hydrodynamic printing of a dielectric elastomer actuator and its application in tunable lenses", *Compos. Part A*, **147**, 106461. https://doi.org/10.1016/j.compositesa.2021.106461

Jiao, J., Ghoreishi, S.M., Moradi, Z. and Oslub, K. (2021), "Coupled particle swarm optimization method with genetic algorithm for the static–dynamic performance of the magneto-electro-elastic nanosystem", *Eng. Comput.*, 1-15. https://doi.org/10.1007/s00366-021-01391-x

Ke, L.L., Liu, C. and Wang, Y.S. (2015), "Free vibration of nonlocal piezoelectric nanoplates under various boundary conditions", *Physica E*, **66**, 93-106. https://doi.org/10.1016/j.physe.2014.10.002

Ke, L.L. and Wang, Y.S. (2012), "Thermoelectric-mechanical vibration of piezoelectric nanobeams based on the nonlocal theory", *Smart Mater. Struct.*, **21**(2), 025018.

https://doi.org/10.1088/0964-1726/21/2/025018
Ke, L.L., Wang, Y.S. and Wang, Z.D. (2012), "Nonlinear vibration of the piezoelectric nanobeams based on the nonlocal theory", *Compos. Struct.*, **94**(6), 2038-2047.
Khanouki, M.M.A., Ramli Sulong, N.H., Shariati, M. and Tahir, M.M. (2016), "Investigation of through beam connection to concrete filled circular steel tube (CFCST) column", *J. Constr. Steel Res.*, **121**, 144-162. https://doi.org/10.1016/j.jcsr.2016.01.002
Kröner, E. (1967), "Elasticity theory of materials with long range cohesive forces", *Int. J. Solids Struct.*, **3**(5), 731-742. https://doi.org/10.1016/0020-7683(67)90049-2
Krumhansl, J. (1968), *Some Considerations of the Relation Between Solid State Physics and Generalized Continuum Mechanics*, Springer.
Kunin, I. (1968), *The Theory of Elastic Media with Microstructure and the Theory of Dislocations*, Springer
Li, D.Y., Toghroli, A., Shariati, M., Sajedi, F., Bui, D.T., Kianmehr, P., Mohamad, E.T. and Khorami, M. (2019), "Application of polymer, silica-fume and crushed rubber in the production of Pervious concrete", *Smart Struct. Syst.*, **23**(2), 207-214. https://doi.org/10.12989/sss.2019.23.2.207
Li, G., Yuan, H., Mou, J., Dai, E., Zhang, H., Li, Z., Zhao, Y., Dai, Y. and Zhang, X. (2022a), "Electrochemical detection of nitrate with carbon nanofibers and copper co-modified carbon fiber electrodes", *Compos. Commun.*, **29**, 101043. https://doi.org/10.1016/j.coco.2021.101043
Li, H., Hou, K., Xu, X., Jia, H., Zhu, L. and Mu, Y. (2022b), "Probabilistic energy flow calculation for regional integrated energy system considering cross-system failures", *Appl. Energy*, **308**, 118326. https://doi.org/10.1016/j.apenergy.2021.118326
Li, J., Tang, F. and Habibi, M. (2020a), "Bi-directional thermal buckling and resonance frequency characteristics of a GNP-reinforced composite nanostructure", *Eng. Comput.*, 1-22. https://doi.org/10.1007/s00366-020-01110-y
Li, Y., Li, S., Guo, K., Fang, X. and Habibi, M. (2020b), "On the modeling of bending responses of graphene-reinforced higher order annular plate via two-dimensional continuum mechanics approach", *Eng. Comput.*, 1-22. https://doi.org/10.1007/s00366-020-01166-w
Li, Z., Peng, X., Hu, G., Zhang, D., Xu, Z., Peng, Y. and Xie, S. (2022c), "Towards real-time self-powered sensing with ample redundant charges by a piezostack-based frequency-converted generator from human motions", *Energy Convers. Manag.*, **258**, 115466. https://doi.org/10.1016/j.enconman.2022.115466
Liu, H., Shen, S., Oslub, K., Habibi, M. and Safarpour, H. (2021a), "Amplitude motion and frequency simulation of a composite viscoelastic microsystem within modified couple stress elasticity", *Eng. Comput.*, 1-15. https://doi.org/10.1007/s00366-021-01316-8
Liu, H., Zhao, Y., Pishbin, M., Habibi, M., Bashir, M. and Issakhov, A. (2021b), "A comprehensive mathematical simulation of the composite size-dependent rotary 3D microsystem via two-dimensional generalized differential quadrature method", *Eng. Comput.*, 1-16. https://doi.org/10.1007/s00366-021-01419-2
Liu, Y., Wang, W., He, T., Moradi, Z. and Larco Benítez, M.A. (2021c), "On the modelling of the vibration behaviors via discrete singular convolution method for a high-order sector annular system", *Eng. Comput.*, 1-23.
Liu, Z., Su, S., Xi, D. and Habibi, M. (2020a), "Vibrational responses of a MHC viscoelastic thick annular plate in thermal environment using GDQ method", *Mech. Based Des. Struct.*, 1-26. https://doi.org/10.1080/15397734.2020.1784201
Liu, Z., Wu, X., Yu, M. and Habibi, M. (2020b), "Large-amplitude dynamical behavior of multilayer graphene platelets reinforced nanocomposite annular plate under thermo-mechanical loadings", *Mech. Based Des. Struct.*, 1-25. https://doi.org/10.1080/15397734.2020.1815544
Lori, E.S., Ebrahimi, F., Supeni, E.E.B., Habibi, M. and Safarpour, H. (2020), "The critical voltage of a GPL-reinforced composite microdisk covered with piezoelectric layer", *Eng. Comput.*, 1-20. https://doi.org/10.1007/s00366-020-01004-z
Lu, C., Zhu, R., Yu, F., Jiang, X., Liu, Z., Dong, L., Hua, Q. and Ou, Z. (2021), "Gear rotational speed sensor based on FeCoSiB/Pb (Zr, Ti) O3 magnetoelectric composite", *Measurement*, **168**, 108409. https://doi.org/10.1016/j.measurement.2020.108409
Luo, J., Song, J., Moradi, Z., Safa, M. and Khadimallah, M.A. (2022), "Effect of simultaneous compressive and inertia loads on the bifurcation stability of shear deformable functionally graded annular fabrications reinforced with graphenes", *Eur. J. Mech. A Solids*, 104581. https://doi.org/10.1016/j.euromechsol.2022.104581
Ma, L., Liu, X. and Moradi, Z. "On the chaotic behavior of graphene-reinforced annular systems under harmonic excitation", *Eng. Comput.*, 1-25. https://doi.org/10.1007/s00366-020-01210-9
Matouk, H., Bousahla, A.A., Heireche, H., Bourada, F., Bedia, E., Tounsi, A., Mahmoud, S., Tounsi, A. and Benrahou, K. (2020), "Investigation on hygro-thermal vibration of P-FG and symmetric S-FG nanobeam using integral Timoshenko beam theory", *Adv. Nano Res.*, **8**(4), 293-305. https://doi.org/10.12989/anr.2020.8.4.293
Mehrabi, P., Shariati, M., Kabirifar, K., Jarrah, M., Rasekh, H., Trung, N.T., Shariati, A. and Jahandari, S. (2021), "Effect of pumice powder and nano-clay on the strength and permeability of fiber-reinforced pervious concrete incorporating recycled concrete aggregate", *Constr. Build. Mater.*, **287**, 122652. https://doi.org/10.1016/j.conbuildmat.2021.122652
Michael, M., Meyyazhagan, A., Velayudhannair, K., Pappuswamy, M., Maria, A., Xavier, V., Balasubramanian, B., Baskaran, R., Kamyab, H. and Vasseghian, Y. (2022), "The content of heavy metals in cigarettes and the impact of their leachates on the aquatic ecosystem", *Sustainability*, **14**(8), 4752. https://doi.org/10.3390/su14084752
Moayedi, H., Aliakbarlou, H., Jebeli, M., Noormohammadiarani, O., Habibi, M., Safarpour, H. and Foong, L. (2020a), "Thermal buckling responses of a graphene reinforced composite micropanel structure", *Int. J. Appl. Mech.*, **12**(1), 2050010. https://doi.org/10.1142/S1758825120500106
Moayedi, H., Ebrahimi, F., Habibi, M., Safarpour, H. and Foong, L.K. (2020b), "Application of nonlocal strain–stress gradient theory and GDQEM for thermo-vibration responses of a laminated composite nanoshell", *Eng. Comput.*, 1-16. https://doi.org/10.1007/s00366-020-01002-1
Moayedi, H., Habibi, M., Safarpour, H., Safarpour, M. and Foong, L. (2019), "Buckling and frequency responses of a graphene nanoplatelet reinforced composite microdisk", *Int. J. Appl. Mech.*, **11**(10), 1950102. https://doi.org/10.1142/S1758825119501023
Mohammadgholiha, M., Shokrgozar, A., Habibi, M. and Safarpour, H. (2019), "Buckling and frequency analysis of the nonlocal strain–stress gradient shell reinforced with graphene nanoplatelets", *J. Vib. Control*, **25**(19-20), 2627-2640. https://doi.org/10.1177/1077546319863251
Mohammadi, A., Lashini, H., Habibi, M. and Safarpour, H. (2019), "Influence of viscoelastic foundation on dynamic behaviour of the double walled cylindrical inhomogeneous micro shell using MCST and with the aid of GDQM", *J. Solid Mech.*, **11**(2), 440-453. https://doi.org/10.22034/JSM.2019.665264
Moradi, Z., Davoudi, M., Ebrahimi, F. and Ehyaei, A.F. (2021), "Intelligent wave dispersion control of an inhomogeneous micro-shell using a proportional-derivative smart controller",

Waves Random Complex Med., 1-24. https://doi.org/10.1080/17455030.2021.1926572

Naderi, A., Behdad, S., Fakher, M. and Hosseini-Hashemi, S. (2020), "Vibration analysis of mass nanosensors with considering the axial-flexural coupling based on the two-phase local/nonlocal elasticity", *Mech. Syst. Signal Pr*., **145**, 106931. https://doi.org/10.1016/j.ymssp.2020.106931

Naderi, A., Fakher, M. and Hosseini-Hashemi, S. (2021), "On the local/nonlocal piezoelectric nanobeams: Vibration, buckling, and energy harvesting", *Mech. Syst. Signal Pr*., **151**, 107432. https://doi.org/10.1016/j.ymssp.2020.107432

Naghipour, M., Yousofizinsaz, G. and Shariati, M. (2020), "Experimental study on axial compressive behavior of welded built-up CFT stub columns made by cold-formed sections with different welding lines", *Steel. Compos. Struct*., **34**(3), 347-359. https://doi.org/10.12989/scs.2020.34.3.347

Najaafi, N., Jamali, M., Habibi, M., Sadeghi, S., Jung, D.w. and Nabipour, N. (2020), "Dynamic instability responses of the substructure living biological cells in the cytoplasm environment using stress-strain size-dependent theory", *J. Biomol. Struct. Dyn*., 1-12. https://doi.org/10.1080/07391102.2020.1751297

Navi, B.R., Mohammadimehr, M. and Arani, A.G. (2019), "Active control of three-phase CNT/resin/fiber piezoelectric polymeric nanocomposite porous sandwich microbeam based on sinusoidal shear deformation theory", *Steel. Compos. Struct*., **32**(6), 753-767. https://doi.org/10.12989/scs.2019.32.6.753

Nguyen, D.D., Tran, Q.Q. and Nguyen, D.K. (2017), "New approach to investigate nonlinear dynamic response and vibration of imperfect functionally graded carbon nanotube reinforced composite double curved shallow shells subjected to blast load and temperature", *Aerosp. Sci. Technol*., **71**, 360-372. https://doi.org/10.1016/j.ast.2017.09.031

Oyarhossein, M.A., Alizadeh, A.a., Habibi, M., Makkiabadi, M., Daman, M., Safarpour, H. and Jung, D.W. (2020), "Dynamic response of the nonlocal strain-stress gradient in laminated polymer composites microtubes", *Sci. Rep*., **10**(1), 1-19. https://doi.org/10.1038/s41598-020-61855-w

Peng, Y., Xu, Z., Wang, M., Li, Z., Peng, J., Luo, J., Xie, S., Pu, H. and Yang, Z. (2021), "Investigation of frequency-up conversion effect on the performance improvement of stack-based piezoelectric generators", *Renewable Energy*, **172**, 551-563. https://doi.org/10.1016/j.renene.2021.03.064

Polyanin, A.D. and Manzhirov, A.V. (2008), *Handbook of Integral Equations*, CRC press.

Pourjabari, A., Hajilak, Z.E., Mohammadi, A., Habibi, M. and Safarpour, H. (2019), "Effect of porosity on free and forced vibration characteristics of the GPL reinforcement composite nanostructures", *Comput. Math. Appl*., **77**(10), 2608-2626.

Razavian, L., Naghipour, M., Shariati, M. and Safa, M. (2020), "Experimental study of the behavior of composite timber columns confined with hollow rectangular steel sections under compression", *Struct. Eng. Mech*., **74**(1), 145-156. https://doi.org/10.12989/sem.2020.74.1.145

Reddy, J. (2007), "Nonlocal theories for bending, buckling and vibration of beams", *Int. J. Eng. Sci*., **45**(2-8), 288-307. https://doi.org/10.1016/j.ijengsci.2007.04.004

Romano, G. and Barretta, R. (2017), "Nonlocal elasticity in nanobeams: The stress-driven integral model", *Int. J. Eng. Sci*., **115**, 14-27. https://doi.org/10.1016/j.ijengsci.2017.03.002

Romano, G., Barretta, R., Diaco, M. and de Sciarra, F.M. (2017), "Constitutive boundary conditions and paradoxes in nonlocal elastic nanobeams", *Int. J. Mech. Sci*., **121**, 151-156. https://doi.org/10.1016/j.ijmecsci.2016.10.036

Safarpour, H., Ghanizadeh, S.A. and Habibi, M. (2018), "Wave propagation characteristics of a cylindrical laminated composite nanoshell in thermal environment based on the nonlocal strain gradient theory", *Eur. Phys. J. Plus*, **133**(12), 532.

Safarpour, H., Hajilak, Z.E. and Habibi, M. (2019a), "A size-dependent exact theory for thermal buckling, free and forced vibration analysis of temperature dependent FG multilayer GPLRC composite nanostructures restring on elastic foundation", *Int. J. Mech. Mater. Des*., **15**(3), 569-583.

Safarpour, H., Pourghader, J. and Habibi, M. (2019b), "Influence of spring-mass systems on frequency behavior and critical voltage of a high-speed rotating cantilever cylindrical three-dimensional shell coupled with piezoelectric actuator", *J. Vib. Control*, **25**(9), 1543-1557. https://doi.org/10.1177/1077546319828465

Safarpour, M., Ebrahimi, F., Habibi, M. and Safarpour, H. (2020), "On the nonlinear dynamics of a multi-scale hybrid nanocomposite disk", *Eng. Comput*., 1-20. https://doi.org/10.1007/s00366-020-00949-5

Shah, S.N.R., Sulong, N.H.R., Jumaat, M.Z. and Shariati, M. (2016a), "State-of-the-art review on the design and performance of steel pallet rack connections", *Eng. Fail. Anal*., **66**, 240-258. https://doi.org/10.1016/j.engfailanal.2016.04.017

Shah, S.N.R., Sulong, N.H.R., Khan, R., Jumaat, M.Z. and Shariati, M. (2016b), "Behavior of industrial steel rack connections", *Mech. Syst. Signal Pr*., **70-71**, 725-740. https://doi.org/10.1016/j.ymssp.2015.08.026

Shah, S.N.R., Sulong, N.H.R., Shariati, M. and Jumaat, M.Z. (2015), "Steel rack connections: Identification of most influential factors and a comparison of stiffness design methods", *Plos One*, **10**(10), e0139422. https://doi.org/10.1371/journal.pone.0139422

Shao, Y., Zhao, Y., Gao, J. and Habibi, M. (2021), "Energy absorption of the strengthened viscoelastic multi-curved composite panel under friction force", *Arch. Civil Mech. Eng*., **21**(4), 1-29. https://doi.org/10.1007/s43452-021-00279-3

Shariati, A., Habibi, M., Tounsi, A., Safarpour, H. and Safa, M. (2020a), "Application of exact continuum size-dependent theory for stability and frequency analysis of a curved cantilevered microtubule by considering viscoelastic properties", *Eng. Comput*., 1-20. https://doi.org/10.1007/s00366-020-01024-9

Shariati, A., Mohammad-Sedighi, H., Żur, K.K., Habibi, M. and Safa, M. (2020b), "On the vibrations and stability of moving viscoelastic axially functionally graded nanobeams", *Materials*, **13**(7), 1707. https://doi.org/10.3390/ma13071707

Shariati, A., Mohammad-Sedighi, H., Żur, K.K., Habibi, M. and Safa, M. (2020c), "Stability and dynamics of viscoelastic moving rayleigh beams with an asymmetrical distribution of material parameters", *Symmetry*, **12**(4), 586. https://doi.org/10.3390/sym12040586

Shariati, M. (2008), *Assessment Building Using None-destructive Test Techniques (ultra Sonic Pulse Velocity and Schmidt Rebound Hammer)*, Universiti Putra Malaysia

Shariati, M., Ghorbani, M., Naghipour, M., Alinejad, N. and Toghroli, A. (2020d), "The effect of RBS connection on energy absorption in tall buildings with braced tube frame system", *Steel. Compos. Struct*., **34**(3), 393. https://doi.org/10.12989/scs.2020.34.3.393

Shariati, M., Heyrati, A., Zandi, Y., Laka, H., Toghroli, A., Kianmehr, P., Safa, M., Salih, M.N.A. and Poi-Ngian, S. (2019), "Application of waste tire rubber aggregate in porous concrete", *Smart Struct. Syst*., **24**(4), 553-566. https://doi.org/10.12989/sss.2019.24.4.553

Shariati, M., Ramli Sulong, N.H., Sinaei, H., Arabnejad Khanouki, M.M. and Shafigh, P. (2011), "Behavior of channel shear connectors in normal and light weight aggregate concrete (experimental and analytical study)", *Adv. Mater. Res*., **168**, 2303-2307. https://doi.org/10.4028/www.scientific.net/AMR.168-170.2303

Shariati, M., Tahir, M.M., Wee, T.C., Shah, S.N.R., Jalali, A.,

Abdullahi, M.M. and Khorami, M. (2018), "Experimental investigations on monotonic and cyclic behavior of steel pallet rack connections", *Eng. Fail. Anal.*, **85**, 149-166. https://doi.org/10.1016/j.engfailanal.2017.08.014

Shen, Z., Zhang, J., Wu, S., Luo, X., Jenkins, B.M., Moody, M.P., Lozano-Perez, S. and Zeng, X. (2022), "Microstructure understanding of high Cr-Ni austenitic steel corrosion in high-temperature steam", *Acta Materialia*, 117634. https://doi.org/10.1016/j.actamat.2022.117634

Shi, D., Chen, Y., Li, Z., Dong, S., Li, L., Hou, M., Liu, H., Zhao, S., Chen, X. and Wong, C.P. (2022), "Anisotropic charge transport enabling high-throughput and high-aspect-ratio wet etching of silicon carbide", *Small Methods*, 2200329. https://doi.org/10.1002/smtd.202200329

Shokrgozar, A., Safarpour, H. and Habibi, M. (2020), "Influence of system parameters on buckling and frequency analysis of a spinning cantilever cylindrical 3D shell coupled with piezoelectric actuator", *Proceedings of the Institution of Mechanical Engineers, Part C: Journal of Mechanical Engineering Science*, **234**(2), 512-529. https://doi.org/10.1177/0954406219883312

Toghroli, A., Mehrabi, P., Shariati, M., Trung, N.T., Jahandari, S. and Rasekh, H. (2020), "Evaluating the use of recycled concrete aggregate and pozzolanic additives in fiber-reinforced pervious concrete with industrial and recycled fibers", *Constr. Build. Mater.*, **252**, 118997. https://doi.org/10.1016/j.conbuildmat.2020.118997

Toghroli, A., Shariati, M., Karim, M.R. and Ibrahim, Z. (2017). "Investigation on composite polymer and silica fume–rubber aggregate pervious concrete", *Fifth International Conference on Advances in Civil, Structural and Mechanical Engineering - CSM 2017*, Zurich, Switzerland, September.

Toghroli, A., Shariati, M., Sajedi, F., Ibrahim, Z., Koting, S., Mohamad, E.T. and Khorami, M. (2018), "A review on pavement porous concrete using recycled waste materials", *Smart Struct. Syst.*, **22**(4), 433-440. https://doi.org/10.12989/sss.2018.22.4.433

Wan, Q., Li, Q., Chen, Y., Wang, T.H., He, X., Li, J. and Lin, C. (2004), "Fabrication and ethanol sensing characteristics of ZnO nanowire gas sensors", *Appl. Phys. Lett.*, **84**(18), 3654-3656. https://doi.org/10.1063/1.1738932

Wang, H., Habibi, M., Marzouki, R., Majdi, A., Shariati, M., Denic, N., Zakić, A., Khorami, M., Khadimallah, M.A. and Ebid, A.A.K. (2022a), "Improving the self-healing of cementitious materials with a hydrogel system", *Gels*, **8**(5), 278. https://doi.org/10.3390/gels8050278

Wang, H., Wu, X., Zheng, X. and Yuan, X. (2021), "Virtual voltage vector based model predictive control for a nine-phase open-end winding pmsm with a common DC Bus", *IEEE T. Industr. Electr.*, https://doi.org/10.1109/TIE.2021.3088372

Wang, M., Jiang, C., Zhang, S., Song, X., Tang, Y. and Cheng, H.-M. (2018), "Reversible calcium alloying enables a practical room-temperature rechargeable calcium-ion battery with a high discharge voltage", *Nature Chem.*, **10**(6), 667-672. https://doi.org/10.1038/s41557-018-0045-4

Wang, Q. (2002), "On buckling of column structures with a pair of piezoelectric layers", *Eng. Struct.*, **24**(2), 199-205. https://doi.org/10.1016/S0141-0296(01)00088-8

Wang, Y., Yang, J., Moradi, Z., Safa, M. and Khadimallah, M.A. (2022b), "Nonlinear dynamic analysis of thermally deformed beams subjected to uniform loading resting on nonlinear viscoelastic foundation", *Eur. J. Mech. A Solids*, **95**, 104638. https://doi.org/10.1016/j.euromechsol.2022.104638

Wang, Y., Zhu, X. and Dai, H. (2016), "Exact solutions for the static bending of Euler-Bernoulli beams using Eringen,s two-phase local/nonlocal model", *Aip Adv.*, **6**(8), 085114. https://doi.org/10.1063/1.4961695

Wang, Z., Yu, S., Xiao, Z. and Habibi, M. (2020), "Frequency and buckling responses of a high-speed rotating fiber metal laminated cantilevered microdisk", *Mech. Adv. Mater. Struct.*, 1-14. https://doi.org/10.1080/15376494.2020.1824284

Wang, Z.L. and Song, J. (2006), "Piezoelectric nanogenerators based on zinc oxide nanowire arrays", *Science*, **312**(5771), 242-246. https://doi.org/10.1126/science.1124005

Wu, H., Hu, X., Li, X., Sheng, M., Sheng, X., Lu, X. and Qu, J. (2022), "Large-scale fabrication of flexible EPDM/MXene/PW phase change composites with excellent light-to-thermal conversion efficiency via water-assisted melt blending", *Compos. Part A*, **152**, 106713. https://doi.org/10.1016/j.compositesa.2021.106713

Wu, J. and Habibi, M. (2021), "Dynamic simulation of the ultra-fast-rotating sandwich cantilever disk via finite element and semi-numerical methods", *Eng. Comput.*, 1-17. https://doi.org/10.1007/s00366-021-01396-6

Wu, T. and Liu, G. (2000), "Application of generalized differential quadrature rule to sixth-order differential equations", *Commun. Numer. Methods Eng.*, **16**(11), 777-784. https://doi.org/10.1002/1099-0887(200011)16:11<777::AID-CNM375>3.0.CO,2-6

Xia, W., Du, J., Habibi, M., Shariati, M. and Khadimallah, M.A. (2022), "Application of Chebyshev-based GDQ and Newmark methods to viscothermoelasticity responses of FG composite annular systems", *Eng. Anal. Bound. Elem.*, **143**, 28-42. https://doi.org/10.1016/j.enganabound.2022.06.003

Xie, X. and Chen, D. (2022), "Data-driven dynamic harmonic model for modern household appliances", *Appl. Energy*, **312**, 118759. https://doi.org/10.1016/j.apenergy.2022.118759

Xiong, Q.M., Chen, Z., Huang, J.T., Zhang, M., Song, H., Hou, X.F., Li, X.B. and Feng, Z.J. (2020), "Preparation, structure and mechanical properties of Sialon ceramics by transition metal-catalyzed nitriding reaction", *Rare Metals*, **39**(5), 589-596.

Xu, W., Pan, G., Moradi, Z. and Shafiei, N. (2021), "Nonlinear forced vibration analysis of functionally graded non-uniform cylindrical microbeams applying the semi-analytical solution", *Compos. Struct.*, 114395. https://doi.org/10.1016/j.compstruct.2021.114395

Yan, W., Feng, G., Luo, X., Hu, Y.-Q., Guo, J., Yu, Z., Zhao, Z. and Ding, S. (2022), "Singlet oxygen-promoted one-pot synthesis of highly ordered mesoporous silica materials via the radical route", *Green Chem.*, **24**(12), 4778-4782. https://doi.org/10.1039/D2GC00869F

Yang, N., Moradi, Z., Khadimallah, M.A. and Arvin, H. (2022), "Application of the Chebyshev–Ritz route in determination of the dynamic instability region boundary for rotating nanocomposite beams reinforced with graphene platelet subjected to a temperature increment", *Eng. Anal. Bound. Elem.*, **139**, 169-179. https://doi.org/10.1016/j.enganabound.2022.03.013

Yu, D., Ma, Z. and Wang, R. (2022a), "Efficient smart grid load balancing via fog and cloud computing", *Math. Probl. Eng.*, **2022**. https://doi.org/10.1155/2022/3151249

Yu, D., Wu, J., Wang, W. and Gu, B. (2022b), "Optimal performance of hybrid energy system in the presence of electrical and heat storage systems under uncertainties using stochastic p-robust optimization technique", *Sust. Cities Soc.*, **83**, 103935. https://doi.org/10.1016/j.scs.2022.103935

Yu, X., Maalla, A. and Moradi, Z. (2022c), "Electroelastic high-order computational continuum strategy for critical voltage and frequency of piezoelectric NEMS via modified multi-physical couple stress theory", *Mech. Syst. Signal Pr.*, **165**, 108373.

Zare, R., Najaafi, N., Habibi, M., Ebrahimi, F. and Safarpour, H. (2020), "Influence of imperfection on the smart control frequency characteristics of a cylindrical sensor-actuator GPLRC cylindrical shell using a proportional-derivative smart

controller", *Smart Struct. Syst.*, **26**(4), 469-480. https://doi.org/10.12989/sss.2020.26.4.469

Zhang, L., Zhang, H. and Cai, G. (2022), "The multi-class fault diagnosis of wind turbine bearing based on multi-source signal fusion and deep learning generative model", *IEEE T Instr. Measur.*, **71**, 1-12. https://doi.org/10.1109/TIM.2022.3178483

Zhang, X., Tang, Y., Zhang, F. and Lee, C.S. (2016), "A novel aluminum–graphite dual-ion battery", *Adv. Energy Mater.*, **6**(11), 1502588.

Zhang, Y., Wang, Z., Tazeddinova, D., Ebrahimi, F., Habibi, M. and Safarpour, H. (2021), "Enhancing active vibration control performances in a smart rotary sandwich thick nanostructure conveying viscous fluid flow by a PD controller", *Waves Random Complex Med.*, 1-24. https://doi.org/10.1080/17455030.2021.1948627

Zhao, Y., Moradi, Z., Davoudi, M. and Zhuang, J. "Bending and stress responses of the hybrid axisymmetric system via state-space method and 3D-elasticity theory", *Eng. Comput.*, 1-23. https://doi.org/10.1007/s00366-020-01242-1

Zhou, C., Zhao, Y., Zhang, J., Fang, Y. and Habibi, M. (2020), "Vibrational characteristics of multi-phase nanocomposite reinforced circular/annular system", *Adv. Nano Res.*, **9**(4), 295-307. https://doi.org/10.12989/anr.2020.9.4.295

Zhou, H., Xu, C., Lu, C., Jiang, X., Zhang, Z., Wang, J., Xiao, X., Xin, M. and Wang, L. (2021), "Investigation of transient magnetoelectric response of magnetostrictive/piezoelectric composite applicable for lightning current sensing", *Sensors Actuat. A Phys.*, **329**, 112789. https://doi.org/10.1016/j.sna.2021.112789

Zhou, J., Bai, J. and Liu, Y. (2022), "Fabrication and modeling of matching system for air-coupled transducer", *Micromachines*, **13**(5), 781.

Zhou, Z.G., Du, S.Y. and Wu, L.Z. (2007), "Investigation of anti-plane shear behavior of a Griffith permeable crack in functionally graded piezoelectric materials by use of the non-local theory", *Compos. Struct.*, **78**(4), 575-583. https://doi.org/10.1016/j.compstruct.2005.11.020

Zhou, Z.-G. and Wang, B. (2002), "The scattering of harmonic elastic anti-plane shear waves by a Griffith crack in a piezoelectric material plane by using the non-local theory", *Int. J. Eng. Sci.*, **40**(3), 303-317. https://doi.org/10.1016/S0020-7225(01)00069-6

Zhou, Z.G., Wu, L.Z. and Du, S.Y. (2006), "Non-local theory solution for a Mode I crack in piezoelectric materials", *Eur. J. Mech. A Solids*, **25**(5), 793-807. https://doi.org/10.1016/j.euromechsol.2005.10.003

Zhu, X. and Li, L. (2017), "Longitudinal and torsional vibrations of size-dependent rods via nonlocal integral elasticity", *Int. J. Mech. Sci.*, **133**, 639-650. https://doi.org/10.1016/j.ijmecsci.2017.09.030

Zhu, X., Wang, Y. and Dai, H.H. (2017), "Buckling analysis of Euler–Bernoulli beams using Eringen,s two-phase nonlocal model", *Int. J. Eng. Sci.*, **116**, 130-140. https://doi.org/10.1016/j.ijengsci.2017.03.008